EUROPEAN SOUTHERN OBSERVATORY

Organisation Européenne pour des Recherches Astronomiques dans l'Hémisphère Austral

Europäische Organisation für astronomische Forschung in der südlichen Hemisphäre

VERY LARGE TELESCOPE

SKYCORR sky correction:
User documentation and evaluation

VLT–MAN–ESO–19550–5896

Issue 4.4

Date 2014–04–01

Prepared:	Innsbruck ESO In-Kind Team	2014-04-01	
	Name	Date	Signature
Approved:	***TBD***		
	Name	Date	Signature
Released:	***TBD***		
	Name	Date	Signature

This page was intentionally left blank

Change record

Issue/Rev.	Date	Section/Parag. affected	Reason/Initiation/Documents/Remarks
4.4	01/04/2014	Sect. 3	Update installation instructions
4.3	20/09/2013	All	RIXes for final review considered
4.2	30/07/2013	All	Changes related to code-testing workshop
			Sky model update
4.1	13/05/2013	Sect. 4 and 5.2	Parameter description, routine extract1D, examples
4.0	30/04/2013	All	Focus on C code, extended I/O options
3.4	03/05/2012	Sect. 4.2 and 5	Description of conversion of FITS 1D images
			Update of the Reflex workflow description
3.3	16/03/2012	Sect. 3, 4, 6	Some rephrasing, Figs. 24-29 changed
3.2	09/03/2012	Sect. 3.2, 4.6, 4.7	Updating installation and running procedure
3.1	18/11/2011	Sect. 6.4 and 7	Update related to line list change
3.0	08/09/2011	All	General update
2.0	31/07/2011	All	General update
1.0	01/06/2011	All	First version

Main authors (Austrian ESO In-Kind Team Innsbruck)

Wolfgang Kausch
Stefan Noll
Marco Barden
Cezary Szyszka
Amy M. Jones
Stefan Kimeswenger

Institute for Astro- and Particle Physics, University of Innsbruck
Technikerstr. 25/8
A-6020 Innsbruck / Austria

This page was intentionally left blank

		Doc:	VLT–MAN–ESO–19550–5896
ESO	SKYCORR sky correction:	Issue:	Issue 4.4
	User documentation and evaluation	Date:	Date 2014–04–01
		Page:	5 of 70

Contents

		Doc:	VLT–MAN–ESO–19550–5896
ESO	SKYCORR sky correction:	Issue:	Issue 4.4
	User documentation and evaluation	Date:	Date 2014–04–01
		Page:	6 of 70

1 Introduction

This document is intended to be a user documentation/manual of the sky correction code SKYCORR developed within the framework of the Austrian ESO In-Kind SM project as described in the corresponding Statement of Work document [SM-SoW].

The aim of the SKYCORR project is to provide an advanced instrument-independent sky-correction tool that removes sky emission in science spectra by means of sky spectra taken at a different time and sky location. The algorithm adapts a reference sky spectrum to a science spectrum by correcting differences due to temporal and spatial airglow variability and issues related with the instrument or the data reduction[1]. The approach is based on a similar method for SINFONI near-IR spectroscopic data described in Davies [2007].

This document is organised as follows: Section 2 gives a brief overview on the project and the incorporated algorithms. Section 3 provides information on the installation procedure. Section 4 contains a description of how to run the code, the required input parameter file, and the output files. Section 5 explains the adapted sky correction method and the airglow model in detail. Finally, the code performance is evaluated in Section 6 by means of a test data set.

---

[1]For multi-object and integral-field spectroscopy, it could be prudent to correct with a reference sky spectrum taken from the same exposure. In this case, SKYCORR would mainly be used to correct for instrumental effects.

2 Overview

2.1 The Davies method

For spectroscopic instrument set-ups and observing programmes that do not provide pure sky spectra in parallel to the desired object spectra (*e.g.* two-dimensional long-slit spectra where the object does not cover the whole slit), it is necessary to use sky spectra taken at a different time as the science spectra for the sky correction. However, the strong variability of airglow emission on time scales in the order of a few minutes can cause unavoidable sky correction residua. Significant changes in the airglow emission can also be expected for sky position differences in the order of a few degrees or even less depending on the characteristics of possible wave patterns. Moreover, different telescope positions and ambient conditions may cause instrument flexures, which result in shifting of the sky with regard to the science spectrum. Hence, the reference sky spectrum has to be adapted in both, the flux and the wavelength regime, to allow a reasonable sky background correction.

An illustration of this problem and a solution for SINFONI has been described by Davies [2007]. The airglow correction method proposed in this paper is based on applying arbitrary sky spectra to science spectra by scaling physically related OH line groups of the sky spectrum to the corresponding groups in the science spectrum. Subsequently, the newly created scaled spectrum is used for the sky correction. Specifically, the Davies method groups emission lines from vibrational-rotational transitions resulting from non-thermal excitation processes of the OH molecule and defines wavelength regions where these groups dominate the airglow emission. These wavelength ranges are scaled in the sky spectrum to match the corresponding flux in the object spectrum. This approach only works for the line component of the sky emission. Since object and sky continua cannot satisfyingly be separated, the sky continuum cannot be adapted and has to be subtracted before the scaling procedure for the line emission can start. Since the Davies method is restricted to OH airglow lines beyond $1\,\mu m^2$, it can only be applied in near-IR wavelength regions where other line emission is negligible. This method has been implemented for SINFONI (Modigliani et al. [2007]).

2.2 Improvements of the Davies method

In the framework of the SM subproject "Advanced sky model", an extended semi-empirical model for airglow emission was developed (see [SM-01] User Manual and Noll et al. [2012]). It is based on the OH line list by Rousselot et al. [2000]. Also, it incorporates the empirical –mainly optical– line list by Hanuschik [2003] and Cosby et al. [2006] based on high-resolution UVES observations, and the HITRAN database for molecular data [3]. Additionally, five variability classes were introduced for the entire line list (*i.e.* green O I, Na D, red O I, OH, and O_2, see Section 5.4) in order to take into account intensity variations due to changes of the solar activity, the season, and the time during the night. The variability correction recipes for the different classes were calculated from 1189 VLT FORS sky spectra (Patat [2008]).

For SKYCORR, this model is extended by identifications of lines with similar upper and lower electronic, vibrational, and/or rotational states that are expected to vary in a very similar way (more similar than the lines belonging to the relatively rough variability classes defined in Noll et al. [2012]). If the spectral resolution is given, the airglow emission model with the improved line list (ranging from 0.3 to $2.5\,\mu m$) allows deriving the contributions of different line groups to the pixels of a sky spectrum. Hence, in wavelength space overlapping

---

[2] The version 2.0 of Davies' code also allows simple scaling of the strong O_2 band at $1.27\,\mu m$. This feature is not described in Davies [2007].

groups can be handled by such an implementation contrary to the Davies method, which uses fixed wavelength intervals. The optimum scaling of the different line groups is then derived by means of a fitting procedure that is not required for the simpler approach of Davies. This fitting procedure also allows the wavelength grid to be adapted. Similar to [MOLECFIT], the adaptation process is based on Chebyshev polynomials and subpixel shifts instead of simple shifting by full pixels only. In general, the new method should be applicable to all wavelength regions where airglow emission plays an important role. Hence, apart from SINFONI, the SKYCORR code is also appropriate for correcting spectroscopic observational data from, *e.g.*, ISAAC, X-Shooter, VIMOS, or FORS.

2.3   Algorithm

The algorithm used by the SKYCORR code is sketched in Figure 1. Its main purpose is the removal of sky emission lines in a science spectrum by means of a scaled reference sky spectrum. To this end, any continuum flux in the input science and reference sky spectra has to be removed in advance. Hence, as a first step, pixels belonging to lines and continuum have to be identified, separated, and masked accordingly. The second step is a fit to continuum pixels only, which is subtracted from the input spectrum to obtain a continuum-free spectrum. In the third step, a weight mask for the different airglow line groups in the reference sky spectrum is calculated incorporating the extended sky model mentioned above. The actual line and wavelength fitting process is performed in step four (incorporating the MPFIT library [1]). Here, the reference sky line spectrum is fitted to the emission lines in the science spectrum. Finally, the best-fit sky line spectrum and the uncorrected sky continuum spectrum are subtracted from the input science spectrum. More details on this approach can be found in Section 5.

	SKYCORR sky correction:	Doc:	VLT–MAN–ESO–19550–5896
ESO	User documentation and evaluation	Issue:	Issue 4.4
		Date:	Date 2014–04–01
		Page:	10 of 70

Figure 1: *Overview of the SKYCORR project workflow.*

		Doc:	VLT–MAN–ESO–19550–5896
ESO	SKYCORR sky correction:	Issue:	Issue 4.4
	User documentation and evaluation	Date:	Date 2014–04–01
		Page:	11 of 70

3 Installation procedure

3.1 Requirements

The installation of the basic SKYCORR binary package requires:

- C99 compatible compiler (e.g. gcc or clang)

- glibc 2.11 or newer on Linux or OS X 10.7 or newer

- common unix utilities (bash, tar, sed, grep, . . .)

The optional GUI to SKYCORR requires:

- Python v2.6 or v2.7 (but not Python v3.x)

- wxPython v2.8 or newer

- Python matplotlib v1.0 or newer

- PyFITS v2.4 or newer

The command line client also has optional display features which require:

- gnuplot v4.2 patchlevel 3 or newer

3.2 Binary installation

First the downloaded installer needs to be made executable. To do this change into the directory the installer was downloaded to and run following command (replacing `skycorr_installer.run` with the actual downloaded filename):

```
chmod u+x ./skycorr_installer.run
```

Now the installer can be executed from the same folder with:

```
./skycorr_installer.run
```

It will ask for an installation directory where it will extract its contents to. It is recommended to choose an empty directory to avoid overwriting existing files.

After the installer has successfully finished, the `skycorr` executables are installed into the `bin` subdirectory of the chosen installation folder. They can be executed by specifying the full or relative path. Also installed are a set of example parameter files for several instruments in the `examples/config` directory. To run a SINFONI example type:

```
<INST_DIR>/bin/skycorr <INST_DIR>/examples/config/sctest_sinfo_H.par
```

For more details see Section 4.

The following directory structure is created by the installation routine:

```
<INST_DIR>
      |
      |-- bin
      |-- config
      |-- doc
      |-- examples
      |       |-- config
      |       |-- data
      |       |-- sysdata -> <INST_DIR>/sysdata/
      |-- output
      |-- sysdata
```

In detail:

- `bin/`: location of binary files

- `config/`: directory containing template configuration files

- `doc/`: documentation

- `examples/`: directory with examples

- `output/`: default output directory

- `sysdata/`: directory containing data required for SKYCORR

3.3 GUI dependencies

The GUI requires some additional dependencies to be installed on the system. To check if the python installation is able to run the GUI, following commands can be run:

```
python -c 'import wx'

python -c 'import matplotlib; import matplotlib.backends.backend_wxagg'

python -c 'import pyfits'
```

If these commands fail please see following site for instructions on how to install these packages:

```
http://www.eso.org/pipelines/reflex_workflows/
```

3.4 Package contents

The installation package is a self extracting tarball containing the SKYCORR source code and pre-built versions of its third party dependencies:

- Common Pipeline Library v6.4.2 and its dependencies cfitsio v3.350, wcslib v4.16 and fftw3 v3.3.3 [7]

3.5 Source Installation

Advanced users may want to install everything from source, the basic instructions for this are outlined in this section.

3.5.1 CPL compilation

The CPL sources can be obtained from [7]

CPL only requires cfitsio in order to run SKYCORR. It can be installed as follows:

```
./configure --prefix=/install-location

make

make shared

make install
```

Then CPL can be install with:

```
./configure --prefix=/install-location --with-cfitsio=/install-location

make

make install
```

See the respective packages documentation for details on the installation procedure.

3.5.2 SKYCORR compilation

After all dependencies have been installed SKYCORR can be compiled from source into the same location.

This is the only step required if one wants to update SKYCORR from source after previously installing the third party dependencies with the binary installer.

		Doc:	VLT–MAN–ESO–19550–5896
ESO	SKYCORR sky correction:	Issue:	Issue 4.4
	User documentation and evaluation	Date:	Date 2014–04–01
		Page:	14 of 70

```
./configure --prefix=/install-location --with-cpl=/install-location
```

```
make
```

```
make install
```

In order to use SKYCORR from this location the environment variable `LD_LIBRARY_PATH` (or `DYLD_LIBRARY_PATH` on Mac OS) need to be set. With the bash shell this is done with following command:

```
export LD_LIBRARY_PATH=/install-location/lib
```

Now `skycorr` is ready to be used from `/install-location/bin`.

4 Code execution procedure

This section describes how to use the SKYCORR software. Section 4.1 provides an example for an input parameter file. The input parameters are discussed in detail in Section 4.2. Finally, the output of the code is described in Section 4.3. In Section 4.4 the execution of the programme is shown. For the extraction of 1D spectra suitable for SKYCORR from 2D FITS images, see Section 4.5. The run of examples is described in Section 4.6. The SKYCORR software also provides a Reflex workflow. It is discussed in Section 4.7.

4.1 Input parameter file

All parameters needed for the fit are read from an ASCII parameter file, which contains parameter names, descriptions, and initial values. In the following, src/test/config/sctest_sinfo_H.par is shown as an example of a parameter file. Individual parameters are explained in Section 4.2:

```
# --------------------------------------------------------------------------
# ------------------- INPUT PARAMETER FILE FOR SKYCORR ---------------------
# --------------------------------------------------------------------------

# -------------------------DIRECTORIES + FILES-------------------------------

# Absolute path of skycorr installation directory
INST_DIR=../../

# Absolute or relative (with respect to INST_DIR) path and filename of input
# object spectrum
INPUT_OBJECT_SPECTRUM=src/test/data/sky_sinfo_1.fits

# Absolute or relative (with respect to INST_DIR) path and filename of input
# sky spectrum
INPUT_SKY_SPECTRUM=src/test/data/sky_sinfo_2.fits

# Absolute or relative (with respect to INST_DIR) path and filename of output
# directory (will be created if not present; default: <INST_DIR>/output/)
OUTPUT_DIR=output

# Main name of diagnostic output files, extensions will be added
OUTPUT_NAME=TEST-SINFO-H

#----------------------------INPUT STRUCTURE-------------------------------

# Names of file columns (table) or extensions (image)
# A list of 4 labels has to be provided:
# 1: wavelength [image: NONE if dedicated extension does not exist]
# 2: flux [image: NONE if in zeroth, unnamed extension]
# 3: flux error [NONE if not present]
# 4: mask (integer: 1 = selected, 0 = rejected;
#          float:  0. = selected, otherwise rejected) [NONE if not present]
COL_NAMES=lambda flux NONE NONE
```

```
# Error relative to mean if no error column is provided (default: 0.01)
DEFAULT_ERROR=0.01

# Multiplicative factor to convert wavelength to micron
# e.g.: wavelength unit = A -> WLG_TO_MICRON = 1e-4
WLG_TO_MICRON=1.

# Wavelengths in vacuum (= vac) or air (= air)
VAC_AIR=vac


# -----------------------------------------------------------------------------
# ---------------------- EXPERT MODE PARAMETERS ---------------------------
# -----------------------------------------------------------------------------


# ----------------------------FITS KEYWORDS-------------------------------

# FITS keyword of sky spectrum for Modified Julian Day (MJD) or date in years
# (default: MJD-OBS; optional parameter for value: DATE_VAL)
DATE_KEY=MJD-OBS

# FITS keyword of sky spectrum for UTC time in s
# (default: TM-START; optional parameter for value: TIME_VAL)
TIME_KEY=TM-START

# FITS keyword of sky spectrum for telescope altitude angle in deg
# (default: ESO TEL ALT; optional parameter for value: TELALT_VAL)
TELALT_KEY=ESO TEL ALT

# --------------------------REQUIRED INPUT DATA----------------------------

# Airglow line list
# Required directory: <INST_DIR>/sysdata/
LINETABNAME=airglow_groups.dat

# File for airglow scaling parameters
# Required directory: <INST_DIR>/sysdata/
VARDATNAME=airglow_var.dat

# FTP address (supplemented by "ftp://") for folder with monthly averages of
# solar radio flux at 10.7 cm
SOLDATURL=ftp.geolab.nrcan.gc.ca/data/solar_flux/monthly_averages

# File with monthly averages of solar radio flux at 10.7 cm
# Required directory: SOLDATURL or <INST_DIR>/sysdata/
SOLDATNAME=solflux_monthly_average.txt

# Solar radio flux at 10.7 cm:
# Positive value in sfu (= 0.01 MJy) or -1 [default] for corresponding monthly
# average from http://www.spaceweather.gc.ca. Download only if local file in
```

```
# <INST_DIR>/sysdata/ does not contain required month.
SOLFLUX=-1


# -------------------------LINE IDENTIFICATION-------------------------

# Initial estimate of line FWHM [pixel]
FWHM=5.0


# Variable line width (linear increase with wavelength)? -- 1 = yes; 0 = no
VARFWHM=0


# Relative FWHM convergence criterion (default: 1e-2)
LTOL=1e-2


# Minimum distance to neighbouring lines for classification as isolated line:
# <MIN_LINE_DIST> * <FWHM> [pixel]
MIN_LINE_DIST=2.5


# Minimum line peak flux for consideration of lines from airglow line list:
# <FLUXLIM> * <median flux of identified lines>
# Automatic search -> FLUXLIM = -1 (default)
FLUXLIM=-1


# -------------------------FITTING OF SKY LINES-------------------------

# Relative chi^2 MPFIT convergence criterion (default: 1e-3)
FTOL=1e-3


# Relative parameter MPFIT convergence criterion (default: 1e-3)
XTOL=1e-3


# Relative chi^2 convergence criterion for iterative improvement of
# wavelength grid (default: 1e-3)
WTOL=1e-3


# Maximum degree of Chebyshev polynomial for wavelength grid correction:
# -1 = no correction
#  0 = linear term (coef. = 1) is also considered but not fitted
#  7 = default
CHEBY_MAX=7


# Minimum degree of Chebyshev polynomial for wavelength grid correction.
# CHEBY_MIN <= CHEBY_MAX:
# - Iterative increase of polynomial degree at least until CHEBY_MIN
#   (default: 3).
# - Procedure stops if chi^2 gets worse or CHEBY_MAX is reached.
# - Results of degree with best chi^2 are taken.
# CHEBY_MIN > CHEBY_MAX:
# - Iterative increase of polynomial degree until CHEBY_MAX is reached.
# - Results of degree CHEBY_MAX are taken.
CHEBY_MIN=3
```

```
# Initial constant term for wavelength grid correction (shift relative to half
# wavelength range)
CHEBY_CONST=0.

# Type of rebinning:
# 0 = simple rebinning (summation of pixel fractions)
# 1 = convolution with asymmetric, damped sinc kernel [default]
REBINTYPE=1

# Minimum relative weight of the strongest line group of a pixel for
# including a pixel in the line fitting procedure (default: 0.67)
WEIGHTLIM=0.67

# Sigma limit for excluding outliers (e.g. object emission lines) from
# estimate of group flux correction factors (default: 15.)
SIGLIM=15.

# Lower relative uncertainty limit for the consideration of a line group for
# the fitting procedure. The value is compared to the sigma-to-mean ratio of
# the group-specific flux correction factors of the initial estimate
# (default: 0. -> include all fittable line groups).
FITLIM=0.

# --------------------------------PLOTTING--------------------------------

# Diagnostic gnuplot plots:
# Options for output on screen:
# W - wxt terminal
# X - x11 terminal
# N - no screen output [default]
# NOTE: An illustration of the sky subtraction quality is plotted into a PS
#       file in the OUTPUT_DIR folder in any case.
PLOT_TYPE=N
```

4.2 Parameter description

In the following, the individual parameters are explained in more detail in the order as they appear in the parameter file. The file is divided into two parts. The first part contains the parameters which provide the paths, file names, and data structures. They have to be adapted if the input and output data files change. However, the sky correction code can be run without modifying the parameters of the second part, which affect the sky correction optimisation. The modification of these so-called expert mode parameters can improve the sky subtraction provided that the user is willing to run the code several times in order to find the optimal parameter set.

```
Basic parameters:
```

- INST_DIR: Installation directory for the data reduction task. In the case of automatic installation (see Section 3.2), this has to be an absolute path and must be the same as given during the installation procedure.

		Doc:	VLT–MAN–ESO–19550–5896
ESO	SKYCORR sky correction:	Issue:	Issue 4.4
	User documentation and evaluation	Date:	Date 2014–04–01
		Page:	19 of 70

- INPUT_OBJECT_SPECTRUM: Absolute or relative (with respect to INST_DIR) path and name of the input object spectrum for the sky subtraction procedure. Currently, American Standard Code for Information Interchange (ASCII) tables, Flexible Image Transport System (FITS) tables with one table extension, and 1D FITS images are allowed. The number of table columns or FITS file image extensions is not restricted. However, only a single column/extension with flux data can be provided. Corresponding columns/extensions for flux errors and mask values are also possible. See also COL_NAMES.

- INPUT_SKY_SPECTRUM: Absolute or relative (with respect to INST_DIR) path and name of the reference input sky spectrum for the sky subtraction procedure. For the accepted file formats, see INPUT_OBJECT_SPECTRUM.

- OUTPUT_DIR: Absolute or relative (with respect to INST_DIR) path to the output directory. The folder will be created if it does not exist.

- OUTPUT_NAME: Unique name space for output files. The extensions _sci.fits_, _sky.fits_, _fit.fits_, _fit.ps_, and _.res_ are added. See Section 4.3 for more details.

- COL_NAMES: Column names of the two input files containing information on wavelength, flux, flux error, and mask. The latter two are optional and can be disabled by setting them to *NONE*. An example would be the following string: *lambda flux NONE NONE*. *Blanks* are used as column name separators. For ASCII files, which have to provide the columns in the given order, the column names are irrelevant, with the exception of *NONE* input. In the case of FITS images, the given labels are compared to the FITS extension names (keyword "EXTNAME"). If there is no extension name for the spectral flux, it is expected to be present in the first layer of the FITS file (0th extension). In this case, the flux column name has to be set to *NONE*. The name of the wavelength column should also be *NONE*, if the wavelength grid is derived from FITS header keywords. This is the typical situation for FITS images. By default, it is expected that an optional mask has only the values 0 and 1 for rejection and selection, respectively. Alternatively, pixels with a mask value of 0 are selected (reverse definition) if the other values (to be rejected) do not equal 1 and are floating-point numbers.

- DEFAULT_ERROR: Default error relative to the mean in the case of a lacking error column (column name = *NONE*, see previous record).

- WLG_TO_MICRON: Multiplicative factor to convert input wavelength unit to micron. For example, for nm this parameter has to set to 10^{-3}.

- VAC_AIR: Wavelengths of the input spectra in vacuum (*vac*) or air (*air*).

Expert mode parameters:

- DATE_KEY: FITS keyword of INPUT_SKY_SPECTRUM for Modified Julian Day (MJD) or date in years. By default, *MJD-OBS* is taken. If ASCII files are provided or no suitable FITS keyword is available, the information has to be provided manually (see below).

- DATE_VAL: MJD or date in years for INPUT_SKY_SPECTRUM. This parameter is only required if a suitable FITS header is not provided by the input spectrum.

- TIME_KEY: FITS keyword of INPUT_SKY_SPECTRUM for UTC time in seconds. By default, *TM-START* is taken. If *TM-START* is not available, an equivalent keyword could be *UTC*. If ASCII files are provided or no suitable FITS keyword is available, the information has to be provided manually (see below).

- TIME_VAL: UTC time in seconds for INPUT_SKY_SPECTRUM. This parameter is only required if a suitable FITS header is not provided by the input spectrum.

- TELALT_KEY: FITS keyword of INPUT_SKY_SPECTRUM for telescope altitude angle in deg. By default, *ESO TEL ALT* is taken. If ASCII files are provided or no suitable FITS keyword is available, the information has to be provided manually (see below).

- TELALT_VAL: Telescope altitude angle in deg for INPUT_SKY_SPECTRUM. This parameter is only required if a suitable FITS header is not provided by the input spectrum.

- LINETABNAME: Name of the input airglow line list. The file must be located in the directory `<inst_dir>/sysdata`.

- VARDATNAME: File for the scaling parameters of the airglow variability model described in Section 5.4. The file must be located in the directory `<inst_dir>/ sysdata`.

- SOLDATURL: FTP address (supplemented by *ftp://*) for folder with monthly averages of the solar radio flux at 10.7 cm. Currently, the link is provided by `www.spaceweather.gc.ca` and can be obtained via ftp by `ftp.geolab.nrcan.gc.ca/data/solar_flux/monthly_averages`.

- SOLDATNAME: Name of file with monthly averages of the solar radio flux at 10.7 cm. The file must be located in the directory `<inst_dir>/sysdata`. The radio flux is taken from the column *obsflux*. If the data for the required month (as derived from the FITS header) is not present in the local file, the latter is substituted by the most recent file of the same name in the remote SOLDATURL folder. In the case of errors a solar radio flux of 130 sfu is assumed, which corresponds to the mean of the solar cycles 19 to 23.

- SOLFLUX: Solar radio flux at 10.7 cm in sfu (= 0.01 MJy). The default value of -1 results in using the corresponding monthly average from the file SOLDATNAME.

- FWHM: Initial guess for the FWHM of the airglow lines in pixels. This start value is improved by an iterative approach (see Section 5.2). The width of the sky lines is required for line identification as well as for the computation of the airglow model.

- VARFWHM: Flag for selecting a constant (= 0) or a variable line width (= 1). In the latter case, all FWHM values are related to the central wavelength of the full wavelength range. The variable FWHM increases linearly with wavelength, *i.e.* the resolution is constant. X-Shooter Echelle spectra show this behaviour. For spectra where the object profile in the slit mainly determines the FWHM, the default constant width option is recommended.

- LTOL: Relative FWHM convergence criterion for iterative derivation of the mean line width in the object and reference sky spectrum (see Section 5.2). The default is 1×10^{-2}. In the case of 1, the code would just use the first FWHM estimate without further iteration.

- MIN_LINE_DIST: Minimum distance to neighbouring lines divided by the FWHM. This factor is required for the line finding algorithm.

- FLUXLIM: Minimum line peak flux for including lines from the airglow line list LINETABNAME in the fit. The given value is multiplied by the median flux of the lines directly identified in the spectrum (see Section 5.1). The default value of -1 indicates an iterative approach for the selection of line list entries that aims at including as many lines as possible without loosing too many pixels for the continuum

interpolation (see Sections 5.1 and 5.3). If the warnings "no isolated lines found" and "all weights = 0" should appear, it might help to select a FLUXLIM value below the start value 0.005 of the automatic search.

- FTOL: Relative χ^2 convergence criterion of the MPFIT least-squares minimisation algorithm for the adaptation of the reference sky spectrum to the sky in the object spectrum (see Section 5.5). The default is 1×10^{-3}, *i.e.*, if χ^2 changes between two iterations by less than 0.1% the fitting process is stopped.

- XTOL: Relative parameter convergence criterion. XTOL has a similar functionality as FTOL but for the fit parameter values instead of χ^2. The default is 1×10^{-3}.

- WTOL: Relative χ^2 convergence criterion for iterative adaptation of the wavelength grid of the reference sky spectrum to the grid of the object spectrum (see Section 5.6). The degree of the Chebyshev polynomial that is used to correct the wavelength solution is increased by 1 for each new iteration. If the resulting χ^2 does not show a relative improvement of WTOL and more, the convergence is reached and the procedure is stopped if CHEBY_MIN is not larger than the polynomial degree of the ongoing iteration (see below). The default is 1×10^{-3}.

- CHEBY_MAX: Maximum degree of Chebyshev polynomial for refined wavelength solution (see Section 5.6). The special case -1 indicates that no adaptation of the wavelength grid is performed. If a degree of 0 is chosen, the linear term is always applied and taken into account with a coefficient of 1. This value is fixed during the fit and cannot be omitted. The default value is 7.

- CHEBY_MIN: Minimum degree of Chebyshev polynomial for refined wavelength solution (see Section 5.6). The iterative increase of the polynomial degree in the course of the fitting procedure is performed at least until CHEBY_MIN is reached. By default, the minimum degree is 3. If the procedure stops directly after the iteration with a degree of CHEBY_MIN, the results of the iteration with the best χ^2 are taken. Choosing a CHEBY_MIN value higher than CHEBY_MAX (*e.g.* 99) results in keeping the results for CHEBY_MAX, regardless of the fitting results for lower polynomials with potentially better χ^2.

- CHEBY_CONST: Constant term of the Chebyshev polynomial for the wavelength solution. The given value represents a shift relative to half the wavelength range of the input spectrum. By default, 0 is assumed. Since the linear term and the higher terms are set to 1 and 0, respectively, at the beginning, the fitting procedure starts without a wavelength correction if the default setting is used.

- REBINTYPE: Flag specifying the rebinning algorithm for adapting the modified sky spectrum to the input sky spectrum (see Section 5.6). There are two options. For a value of 0 the rebinning is based on a summation of pixel fractions. A value of 1 selects the more sophisticated default rebinning method, which is based on a convolution with a pixel-dependent, asymmetric, damped sinc kernel. The latter method is particularly useful for input spectra with significant (> 0.1 pixels) differences in the wavelength grids.

- WEIGHTLIM: Minimum relative weight of the strongest line group of a pixel for including a pixel in the line fitting procedure (see Section 5.5). The relative threshold can be set to values in the range $0 - 1$. In the former extreme case all spectrum pixels and in the latter case pixels with only a single line group are included in the line flux and wavelength correction procedure. The default value is 0.67, *i.e.*, a pixel is considered if the dominating group is at least twice as strong as the second group. Since the group weights are crude estimates based on the time-dependent airglow model discussed in Section 5.4, the selected cut tends to be diffuse for realistic group weights.

- SIGLIM: σ-limit for excluding outliers (*e.g.* object emission lines) from the sky line fitting procedure. The standard deviation σ is derived from the ratio of the object and sky line peaks. The default value is 15.

- FITLIM: Lower relative limit for the consideration of a line group for the fitting procedure. The initial estimate of the line group scaling factors results in a mean and an RMS scatter for each group. Then, groups are included for fitting if the σ-to-mean ratio is above the provided parameter value. By default FITLIM is 0, which selects all groups with at least one valid line for the fitting procedure. A high value of *e.g.* 100 would avoid the use of MPFIT for the line strength correction. Simple line group scaling would be applied only, which is very fast but tends to be less accurate than the fitting procedure.

- PLOT_TYPE: Optional output of diagnostic plots on the screen using either a wxt (W) or an x11 (X) terminal. The default N indicates that no screen output is produced. Independent of the choice of this parameter a postscript plot with a comparison between the input object spectrum and the best-fit sky spectrum is written to OUTPUT_DIR (see Section 4.3).

4.3 Output files

4.3.1 Output overview

The output files produced by the sky correction code are stored in the directory specified by the OUTPUT_DIR parameter. The following output files (named corresponding to the OUTPUT_NAME parameter) are created:

- <OUTPUT_NAME>_sci.fits: input science spectrum converted into a FITS table. Columns names are taken from COL_NAMES. In the case of *NONE* for wavelength and flux, *LAMBDA* and *FLUX* are taken. Independent of the presence of a mask column in the original data, an integer mask column with 0 for rejection and 1 for selection is added. If a mask column name is available, *_I* is suffixed. Otherwise it is called *MASK_I*.

- <OUTPUT_NAME>_sky.fits: input sky spectrum converted into a FITS table. For details on the column names, see above.

- <OUTPUT_NAME>_fit.fits: full FITS table of the sky correction procedure for diagnostic purposes with the following columns:

  - *lambda*: wavelength of input science spectrum in micron
  - *flux*: flux of input science spectrum
  - *dflux*: flux error of input science spectrum (only present if available)
  - *mask*: integer mask of input science spectrum (only present if available)
  - *weight*: reciprocal of error or 0 for masked pixels in the input science spectrum
  - *class*: flag for line identification (0 = continuum pixel, 1 = line pixel, 2 = line peak, 3 = isolated line peak for FWHM estimation)
  - *cflux*: continuum flux of science spectrum
  - *lflux*: line flux of science spectrum
  - *mcflux*: rebinned continuum flux of reference sky spectrum

		Doc:	VLT–MAN–ESO–19550–5896
ESO	SKYCORR sky correction:	Issue:	Issue 4.4
	User documentation and evaluation	Date:	Date 2014–04–01
		Page:	23 of 70

- – *mlflux*: rebinned line flux of modified reference sky spectrum

- – *mflux*: adapted reference sky spectrum (sum of *mcflux* and *mlflux*)

- – *mdflux*: flux error in adapted reference sky spectrum (only present if available)

- – *mmask*: rebinned integer mask of reference sky spectrum (only present if available)

- – *mweight*: rebinned weight of reference sky spectrum

- – *sigclip*: σ-clipping of pixels depending on ratio of science and sky line flux (0 = no clipping, 1 = clipped)

- – *cweight*: resulting pixel weight combining *weight*, *mweight*, and *sigclip*

- – *dev*: weighted difference between *mlflux* and *lflux* (for χ^2 calculation)

- – *scflux*: sky-subtracted science spectrum (difference between *flux* and *mflux*)

- – *scdflux*: flux error in sky-subtracted science spectrum (only present if available)

- – *scmask*: integer mask of sky-subtracted science spectrum (only present if available)

- • <OUTPUT_NAME>_fit.ps: postscript plot showing a comparison of the best-optimised reference sky spectrum, the input science spectrum, and the difference of both spectra.

- • <OUTPUT_NAME>.res: results file containing information on the quality of the sky correction procedure and the best-fit parameters (see Section 4.3.2).

Apart from the intermediate and diagnostic products, a file with the sky subtraction results is written in OUTPUT_DIR that has the same file format as the input science spectrum. The original file name is complemented by "_SC". In the case of ASCII and FITS tables, the columns *scflux*, *scdflux*, and *scmask* are added to the input data. The latter two columns are only present if flux error and mask columns are already provided by the input file. In the case of a FITS image, the data in the flux extension is substituted by the sky-subtracted flux. Similar operations are performed for optional flux error and mask extensions. If a non-integer mask is provided by the input file, the integer mask values from *scmask* are converted (see also COL_NAMES in Section 4.2). In the case of FITS files, an extended header with keywords related to the sky correction procedure is written into the first FITS layer.

4.3.2 Example of a `.res` file

The <OUTPUT_NAME>.res contains detailed information on the fit results. In particular, information on the fit quality, *i.e.* χ^2 and r.m.s values, the line FWHM estimation, all coefficients of the best-fit model, and their uncertainties are given. For a description of the provided status message, see the documentation in `mpfit.h`. In general, positive numbers imply that the code found a solution. In the case of status 99, no fitting could be performed due to a lack of suitable lines. In this special case, the reference sky spectrum is simply subtracted from the object spectrum.

In the following, the output file belonging to the parameter file listed in Section 4.1 is shown:

```
INPUT DATA FILES:
Science: evaluation/data/sky_sinfo_1.fits
Sky:     evaluation/data/sky_sinfo_2.fits
```

```
MPFIT RESULTS:
Status:                 1
Fit parameters:         27
Data points:            1921
Weight > 0:             510
MPFIT calls:            9
Iterations:             37
Function evaluations:   587
Fit run time in s:      8.08
Initial chi2:           5.229e+04
Best chi2:              3.744e+04
Reduced chi2:           7.768e+01
RMS rel. to error:      8.814e+00
Full RMS:               3.150e+03
Full RMS rel. to peaks: 1.918e-02
Line RMS rel. to peaks: 2.314e-02
Peak RMS rel. to peaks: 2.991e-02
Mean rel. residual:     2.853e-02

ESTIMATED SPECTRAL RESOLUTION:
FWHM in pixels: 3.325

BEST-FIT PARAMETERS:

Type N  Fit     Value               RMS         N_lin
A    30 0       2.333 +- 9.99       9.99        0
A    31 1       2.965 +- 0.0188     0.1124      11
A    32 1       2.528 +- 0.01604    0.03491     23
A    33 1       2.268 +- 0.0144     0.04689     34
A    34 1       1.992 +- 0.01263    0.05744     31
A    35 1        1.84 +- 0.01168    0.05968     22
A    36 0       2.333 +- 9.99       9.99        0
A    47 1       4.494 +- 0.2091     0.8258      18
B    01 1       1.233 +- 0.00794    0.01799     4
B    02 1       1.242 +- 0.007881   0.01401     15
B    03 1       1.217 +- 0.007788   0.01507     8
B    04 1       1.238 +- 0.007854   0.01515     19
B    05 1        1.25 +- 0.007979   0.06325     10
B    06 1       1.248 +- 0.007944   0.02035     16
B    07 1       1.268 +- 0.00823    0.04584     11
B    08 1       1.198 +- 0.007695   0.02138     13
B    09 1       1.118 +- 0.008475   0.02639     5
B    10 1       1.153 +- 0.007893   0.09762     8
B    21 1       1.772 +- 0.0837     0.3374      3
```

```
B      22  1         2.077 +- 0.08977    0.08087    2
B      23  1         1.358 +- 0.06366    0.149      4
B      24  1         2.357 +- 0.1192     0.1241     1
w      00  1  -4.717e-06 +- 3.498e-07    9.99       0
w      01  1             1 +- 1.277e-06  9.99       0
w      02  1   1.017e-05 +- 5.767e-07    9.99       0
w      03  1   8.649e-06 +- 3.823e-07    9.99       0
w      04  1             0 +- 4.689e-07  9.99       0


REMARKS:
Type: A/B = line group A/B, w = wavelength fit coef.
Fit: 1 = free MPFIT par., 0 = only initial estimate
RMS: uncertainty of initial estimate
9.99: no error available
N_lin: number of lines for fitting
```

4.4 Executing SKYCORR

After the installation, the folder `<INST_DIR>/bin/` contains the executable. It is invoked by

```
cd <INST_DIR>/
bin/skycorr <parameter file>
```

where `<parameter file>` represents a user-defined parameter file (including paths).

4.5 Executing `extract1d`

After the installation, the folder `<INST_DIR>/bin/` also contains a programme for the extraction of 1D spectra for SKYCORR from 2D FITS images. The executable `extract1d` was added especially for X-Shooter pipeline spectra, which belong to the set of example data (see Section 4.6).

Since the current X-Shooter pipeline does not produce 1D sky spectra, they have to be extracted from 2D spectra. In order to make sure that the number of extracted sky pixels per wavelength bin is the same for the sky and the science spectrum, the extraction of both 1D frames is performed together. For the extraction, just a fixed pixel range in spatial direction is considered, which is derived by means of the spatial object profile. Only pixels that have at least a minimum flux relative to the full flux range indicated by the profile are selected. By default, this limit is 0.01. It can be changed by modifying the fourth parameter of `extract1d` (see below). If the input FITS files provide an extension with mask or quality values, this is used to avoid bad pixels in the extracted 1D science spectrum. The relative contribution of skipped pixels to the profile function is taken to correct for changes in the extracted 1D science spectrum due to pixel masking. The extraction algorithm for the 1D science spectrum is not as elaborate as the approach used by the X-Shooter pipeline. However, for demonstrating the performance of SKYCORR, it is required to extract science and sky spectra in a consistent way. The 1D sky spectrum is derived from the median flux in spatial direction and then scaled to the effective number of pixels that were used for the extraction of the 1D science spectrum. For a bright and/or extended object, the choice

of a median, *i.e.* taking the pixel at the relative position 0.5 in flux-sorted pixel list, could be not optimal. For this case, the selected relative position in the sorted pixel list can be modified by the fifth input parameter (see below). The values 0.4 or 0.45 could be reasonable for a bright object.

The executable `extract1d` is invoked by

```
cd <INST_DIR>/
bin/extract1d <parameter file>
               <2D FITS image for science spectrum>
               <2D FITS image for sky spectrum>
               <minimum relative profile flux>
               <selected relative position in flux-sorted pixel list>
```

where `<parameter file>` represents a user-defined parameter file (including paths). The two input files must have the same file formats and the instrumental set-up should have been the same. It is possible to use the same FITS file for the science and sky spectrum. In this case, the performance of SKYCORR and the extraction algorithm can be compared with the one of the X-Shooter pipeline (see Section 4.6).

4.6 Executing the sky correction examples

After an automatic installation, a series of example input files is located in the folder `<INST_DIR>/examples/config/`. The corresponding spectra can be found in the subfolder `<INST_DIR>/examples/data/`. There are two types of examples in the `examples/config/` folder. The names of the parameter files of the first type start with `sctest`. They comprise examples of spectra from the SINFONI, X-Shooter, and FORS instruments. These examples are a subset of the spectra studied in Section 6. After automatic installation, they can directly be tested by invoking

```
bin/skycorr examples/config/<config_file>
```

in the `<INST_DIR>/` folder. Note that –in case of a manual installation of the software– the paths in the example configuration files have to be edited accordingly in advance.

The parameter files whose names start with `XPL` represent test data from the X-Shooter pipeline (V2.0.0; see Modigliani et al. [2010]) without sky subtraction. Before SKYCORR can be run, the provided 2D FITS images have to be converted into 1D FITS images. For this purpose, the programme `extract1d` can be used (see Section 4.5). The required command-line parameters are provided by the SKYCORR parameter files as comment lines at the beginning. For convenience, the SKYCORR input files produced by `extract1d` can already be found in `examples/config/`. The examples are for all three X-Shooter arms UVB, VIS, and NIR. Set-ups are provided that use the same 2D spectrum for the 1D science and sky spectrum (`d0h`). On the other hand, one can also test the situation when the sky spectrum was taken two hours after the science spectrum (`d2h`). Especially in the case of the `d0h` files, the results can be compared to the sky-subtracted 1D spectra from the pipeline. The corresponding reference files are indicated by `ref` in the file name. A detailed discussion of the X-Shooter examples can be found in the report [SM-03-SR].

(a)   (b)

Figure 2: (a) 'Run' button to start the Reflex workflow; (b) zoom toolbar provided by the Python library `matplotlib`. With the leftmost symbol, the user always comes back to the overview; the second and the third symbol enables the user to go 'Back' and 'Forward' in the zooming history; the 4th button shifts the plot via the mouse; the 5th button is the actual zooming button, which can be used via the mouse; the 6th button opens a window to configure the subplots; the 7th button saves the plot to a file.

4.7 Reflex workflow

The SKYCORR package comes along with a workflow embedded in the Reflex[3] environment. This workflow provides a graphical user interface to provide the parameter settings to the underlying SKYCORR base code, and incorporates a plotting routine. For a detailed description on the usage of Reflex, we refer the reader to the Reflex User Manual [Reflex-UM]. For demonstration purposes, the Reflex workflow is ready to be run with an example after invoking.

The Reflex workflow canvas contains four sections:

- **Input / output paramters**: In this section all required information on the input / output has to be given. In particular, the directory structure, file names, and the properties of the input spectra must be provided here. Note: Do *not* change the installation directory. We also highly recommend not to change the parameters which are marked in light blue. A comprehensive description of the parameters are given in Sections 4.1 and 4.2.

- **Fitting parameters:** In this section the fitting parameters can be modified. A comprehensive description of the parameters are given in Sections 4.1 and 4.2. Note: The parameters are not fully checked for the compatibility with respect to SKYCORR at this stage. If something goes wrong, a Reflex-based error window occurs and shows – apart from the Java messages arising from the underlying Reflex workflow – also the SKYCORR error message.

- **Workflow instructions:** Here, a short description of the workflow is given.

- **Workflow**: Actual Reflex workflow.

After providing all parameters, the workflow can be started by pressing the 'Run' button in the Reflex top menu (see Figure 2(a)). Now, the SKYCORR base code is invoked with a parameter file created on basis of the user-defined parameter set. The usual console output of SKYCORR is suppressed by Reflex, except in case of an error. To watch the progress, we recommend to activate the animation provided by Reflex via its main menu ('Tools' → 'Animate at Runtime' → set value to 1).

After the fit is finished, a plotting window is opened to enable the user to check the results (see Figure 4). This window provides a toolbar in the lower left corner, which enables the user to zoom into details (see Figure 2(b). By exiting the plot windows ('Exit' button) the Reflex workflow is finished and can be invoked again. In this way, a best fit can be achieved iteratively.

---

[3] https://www.eso.org/sci/software/reflex/

Figure 3: Canvas of the SKYCORR Reflex workflow.

Figure 4: Plot of the SKYCORR Reflex workflow.

	SKYCORR sky correction:	Doc:	VLT–MAN–ESO–19550–5896
ESO	User documentation and evaluation	Issue:	Issue 4.4
		Date:	Date 2014–04–01
		Page:	30 of 70

5 Mathematical / physical description

In the following, we describe the SKYCORR sky correction procedure in more detail (also see Section 2.3). First, we discuss how emission lines are identified in the input science and sky spectra (Section 5.1). This procedure also derives the typical line FWHM (Section 5.1). Next, the subtraction of the remaining continua from the identified line spectra is described (Section 5.3). Then, the airglow model is discussed (Section 5.4). It is an essential input for scaling the reference sky line spectrum to fit the science line spectrum (Section 5.5). The fitting procedure also allows adapting the wavelength grids (Section 5.6). The final step of the sky correction procedure is the sky subtraction itself. This operation is just the subtraction of the best-fit sky line spectrum and the unscaled sky continuum spectrum from the input science spectrum (see also Section 2.3).

5.1 Line finder

The sky correction procedure focuses on fitting the airglow emission lines in an input science spectrum by scaling a reference sky line spectrum. Hence, object and sky continua have to be subtracted in advance. This requires identification of line and continuum pixels in the input spectra. Spectral lines are identified by an approach that uses the first derivative of the spectrum. Thus, line pixels can be recognised by their large flux gradients. Emission line peaks can be identified by a change from positive to negative values of the first derivative.

Figure 5 shows the X-Shooter spectrum `sky_xshoo_28` (see Section 6) in the upper panel. A zoom-in to the wavelength range $\lambda = 1.6...1.605\,\mu$m isolates a prominent single emission line (middle panel). The first derivative of the same spectral range (lower panel) reveals a significant change from positive to negative values allowing detection of emission lines. Single emission lines are identified by this particular signature. Note that only changes $\geq 1\sigma$ above the noise level are taken into account to avoid spurious detections from noise or broad lines caused by blending.

Line identification via the first derivative allows robust characterisation of lines also in case of strong (pseudo)-continuum variations. This is necessary as isolated lines are required for estimating their FWHM. Figures 6 and 7 show a SINFONI J-band and H-band spectrum, respectively. In the latter a simulated object spectrum was added to the sky emission (see Section 6 for more information). The distinct emission peak at $\lambda \sim 1.25....1.3\,\mu$m in the J-band is a pseudocontinuum caused by many unresolved O_2 sky lines, whereas in the H-band observation a real continuum is visible. In both cases, individual emission lines could be identified.

All detected lines are assembled in a line list, which is refined by an iterative method depending on the estimation of the sky line FWHM (see Section 5.2). This procedure requires identification of strong, isolated lines. Therefore, the line finder checks the previously identified line peaks, applying criteria characterising isolated lines. For a line to be marked as isolated, it has to be sufficiently separated from other lines and its peak has to have a symmetric shape. The first criterion can be influenced by the user. The parameter file includes the unitless scaling parameter MIN_LINE_DIST that is internally multiplied by the line FWHM in pixels. Also, this parameter is included in the driver file (see Section 4.2). Since the FWHM is optimised in an iterative procedure (see Section 5.2), the given value in the file is only used as first guess.

For strong and well separated lines, the described line finding method is very robust. However, for low resolution spectra with many blended lines a major fraction of lines may be missed. Therefore, the line list of the airglow model is being used (see Section 5.4) to find previously unidentified lines that have fluxes above the median
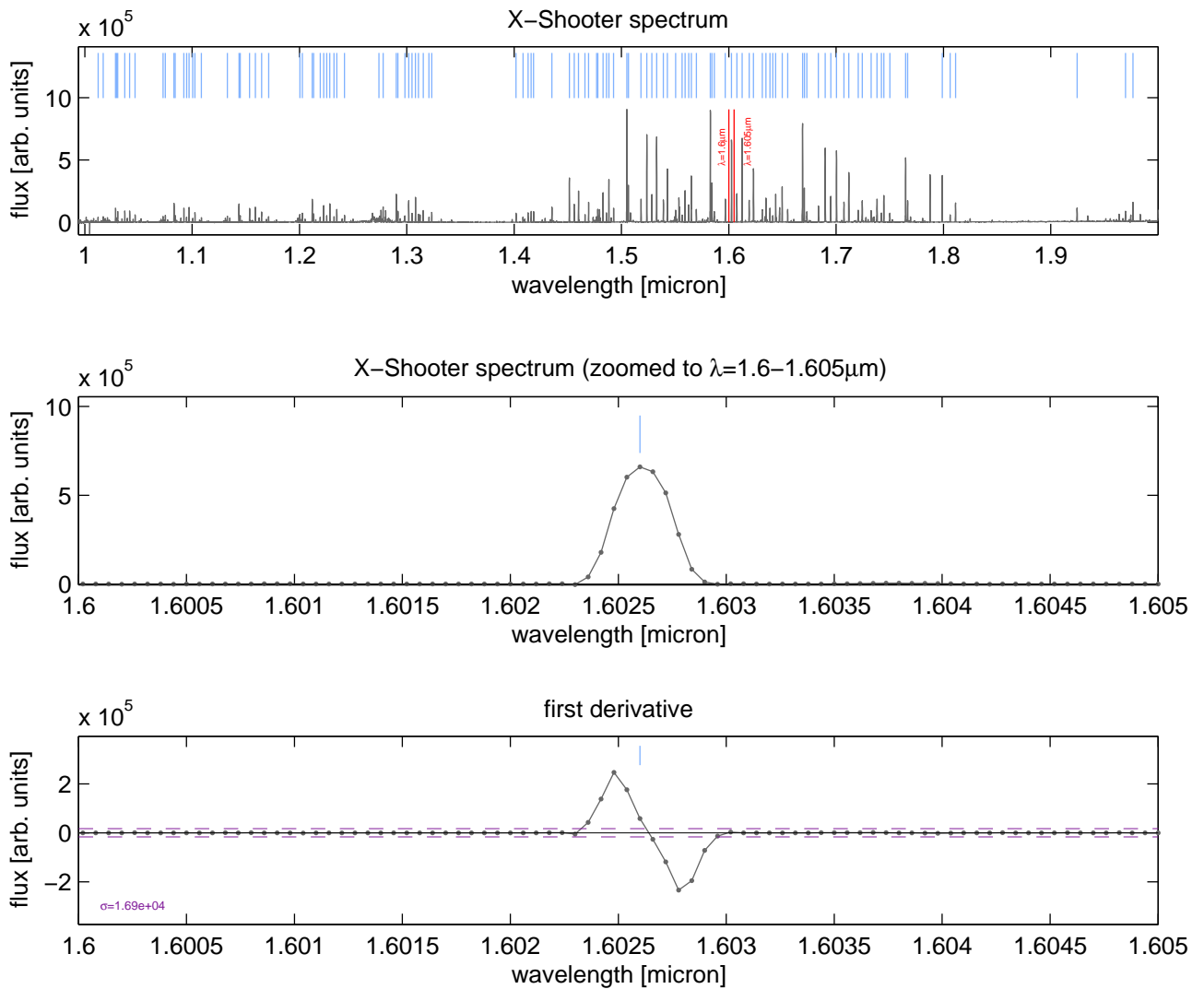
Figure 5: X-Shooter sky spectrum `sky_xshoo_28`. The upper panel shows the entire wavelength range $\lambda = 1.0...2.0\,\mu m$ with the zoom range $\lambda = 1.6...1.605\,\mu m$ (red lines) shown in the middle panel containing a prominent single emission line. In the lower panel the first derivative of this line is given, which shows a significant change in the values. Such changes are used as signature to identify emission lines (marked by the light blue vertical lines in the panels).

		Doc:	VLT–MAN–ESO–19550–5896
ESO	SKYCORR sky correction:	Issue:	Issue 4.4
	User documentation and evaluation	Date:	Date 2014–04–01
		Page:	33 of 70

Figure 6: SINFONI *J*-band sky spectrum with detected emission lines (blue = isolated lines used for the FWHM estimate).
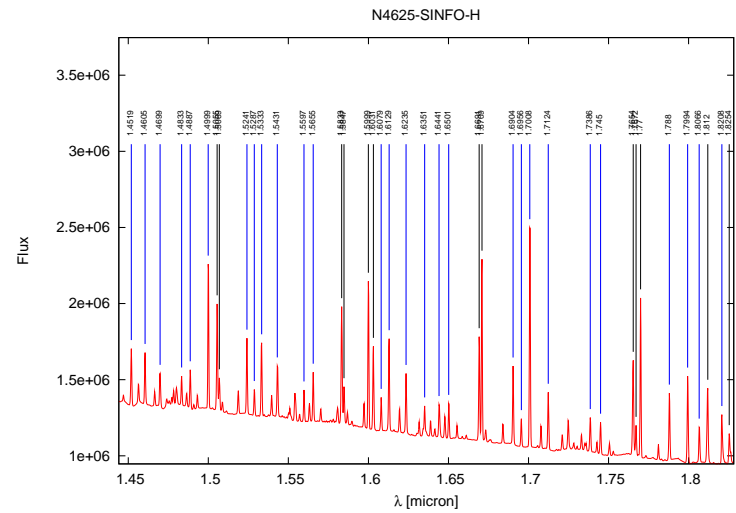
Figure 7: SINFONI *H*-band sky spectrum + arbitrarily scaled NGC 4625 spectrum at $z = 0.5 + 5$ artificial emission lines of equal intensity with detected emission lines (blue = isolated lines used for the FWHM estimate).

Figure 8: Line flags identified in a part of a SINFONI *H*-band spectrum. The meaning of the flags is as follows: 0 = continuum, 1 = line pixel, 2 = line peak, 3 = isolated line peak.

flux of the lines identified by the derivative approach times the FLUXLIM parameter of the parameter file. By default, FLUXLIM is set to -1, which indicates an iterative approach starting with 0.005 and doubling the previous value in subsequent iterations. If the higher limit does not spare sufficient continuum pixels for the continuum interpolation (see Section 5.3), *i.e.* at least 20% of all pixels distributed over more than 90% of the wavelength range, the procedure is stopped and 0.005 is eventually selected, otherwise the threshold value is doubled (*i.e.* 0.02 is taken). This process is repeated as long as a sufficient number of continuum pixels are left over or a value of 0.08 is reached. The number of pixels characterised as line pixels for each line included from the line list depends on the given line FWHM (see above and Section 5.2). The combination of line pixels identified by both methods gives a good estimate of the spectral ranges covered by significant airglow lines (see Figure 8).

5.2 Line FWHM estimator

For calculating the airglow model (see Section 5.4), it is required to convert total line fluxes as provided by the input line list into fluxes per wavelength interval. Consequently, it is necessary to know the typical FWHM of the airglow lines, which is the only line shape parameter assuming a Gaussian line profile. The line finder described in the previous Section 5.1 searches for isolated lines that are suitable for deriving a FWHM. After the subtraction of the continuum (see Section 5.3), the FWHM estimation can be performed by fitting a Gaussian to the line pixels belonging to each isolated line. For the fitting procedure, the C version of the least-squares fitting library MPFIT by C. Markwardt [1] based on the FORTRAN fitting routine MINPACK-1 by Moré et al. [1980] is used (see also Section 5.5). The FWHM measurements of all isolated lines are averaged to obtain the typical FWHM of the input spectrum. In order to avoid blended lines contributing to the resulting mean, a σ-clipping

approach is applied to skip suspiciuosly high FWHM. The method is based on computing the median absolute difference between the data points and their median and the subsequent application of Huber's method for an iterative clipping of outliers [5] and the derivation of reliable mean and standard deviation from the unclipped values. If less than five isolated lines remain after clipping, the median FWHM is taken.

The fact that the estimated value of the FWHM affects the search for isolated lines (see Section 5.1), which are required for the FWHM estimation, necessitates an iterative approach in which line finder, continuum subtractor, and FWHM estimator are called several times in turn in order to obtain a stable and trustworthy FWHM. This iterative procedure is terminated if convergence is reached for the mean FWHM. The convergence criterion is provided by the parameter LTOL (see Section 4.2).

For instruments like X-Shooter, whose spectra show a roughly linear increase of the FWHM with wavelength, this can be considered by the setting the parameter VARFWHM to 1. In this case, the FWHM estimates of the individual lines are converted to correspond to the FWHM, which would be measured at the central wavelength of the full spectrum, assuming a linear change of the FWHM with wavelength. The converted FWHM are then used to calculate the mean FWHM as discussed above. The linear change of the FWHM is also considered for the separation of lines and continuum (see Section 5.1) and the calculation of the pixel contributions of the different line groups (see Section 5.5).

5.3   Continuum subtraction

The adaptation of the reference sky line spectrum to the airglow lines in the input science spectrum by multiplying factors to physically motivated line groups (see Section 5.4) requires that any kind of continuum is subtracted before this procedure. In particular, the object continuum can cause problems, since it is not present in the reference sky spectrum. However, sky spectra also show continuum emission. The main components are scattered moonlight, scattered starlight, zodiacal light, thermal emission from the lower atmosphere by greenhouse gases and the telescope itself, and airglow continuum emission, which is related most probably to chemiluminescent reactions in the upper atmosphere involving nitric oxide (see Section 5.4, Noll et al. [2012], and Khomich et al. [2008] and references therein). As Figure 9 indicates, the main continuum component is the airglow/residual continuum[4], which dominates shortwards of the thermal regime with the exception of the UV and optical if the Moon is up. The variable airglow continuum (see Figure 11) cannot be corrected by a fitting procedure like for the airglow lines (see Section 5.4), since object and sky continuum cannot be separated in the science spectrum (cf. Section 2.1). Therefore, it has to be assumed that the sky continuum in the science spectrum does not differ much from the one in the reference sky spectrum. If this requirement is fulfilled, a simple subtraction of the continua in both input spectra of the sky correction procedure should provide results with good quality.

SKYCORR obtains the continua in the input science and sky spectra using line identification flags (see Figure 8) set in the course of the line search described in Section 5.1. All pixels not flagged as line pixels are connected by linear interpolation. Thorough identification of continuum pixels guaranteed, this is the most efficient approach even in the case of line blends covering wide wavelength ranges.
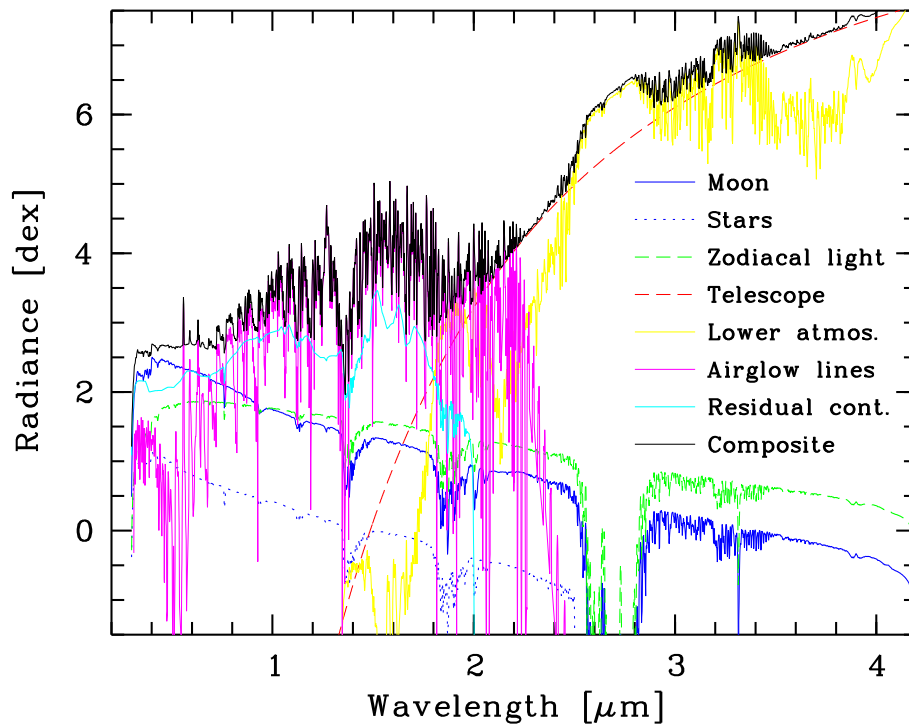
Figure 9: Components of the SM-01 sky model for wavelengths between 0.3 and $6\,\mu$m in logarithmic flux units. The example with Moon above the horizon shows the scattered moonlight, scattered starlight, zodiacal light, thermal emission by telescope and instrument, molecular emission of the lower atmosphere, airglow emission lines of the upper atmosphere, and airglow/residual continuum.

Figure 10: Variability classes for sky emission lines. The following groups are defined: green O I, Na I D, red O I, OH, and O_2. The weak lines (green curves) are scaled by a factor of 30 for Na I D, red O I, and O_2, and a factor of 10 for OH.

	SKYCORR sky correction:	Doc:	VLT–MAN–ESO–19550–5896
ESO	User documentation and evaluation	Issue:	Issue 4.4
		Date:	Date 2014–04–01
		Page:	38 of 70

Figure 11: Variability correction for the five sky line classes and the airglow continuum of the sky model. The variability is shown as a function of the bimonthly period (1 = Dec/Jan, ..., 6 = Oct/Nov), time bin (third of the night), and the solar activity measured by the solar radio flux (sfu = 0.01 MJy).
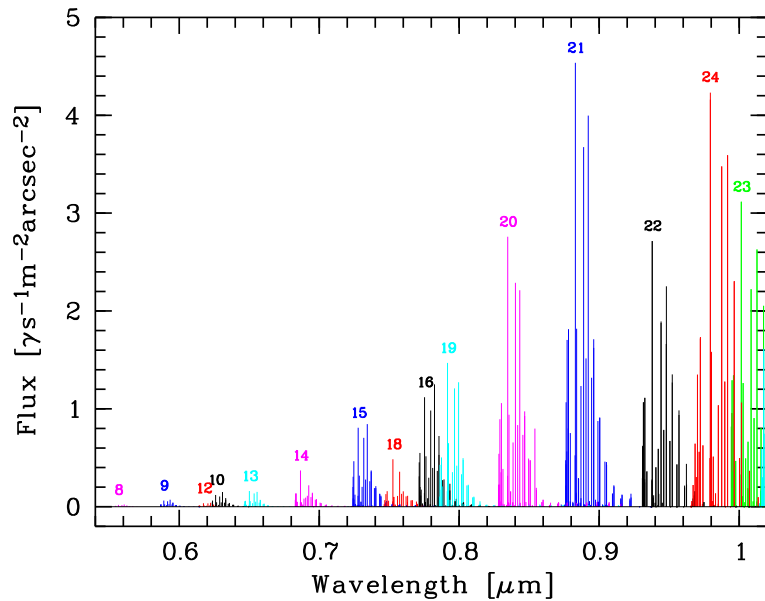

Figure 12: A group identifications of OH bands (cf. Table 1) in the wavelength range between 0.54 and 1.02 μm that have Q1(1.5) lines (see Table 2 and Figure 14) stronger than 0.01 γ s^{-1} m^{-2} arcsec^{-2}. The wavelengths and zenithal mean fluxes (considering absorption in the lower atmosphere) tabulated in the input line list are plotted. Note that the bands with numbers up to 21 appear twice as strong as the bands at longer wavelengths, since the corresponding lines were taken from the Hanuschik [2003] atlas, where OH doublets are often unresolved and are listed as one line only.

Table 1: Description of A groups in the input line list

ID	N_{lin}	Wavelength range [µm]	Description
1	61	0.314 - 0.872	green O I at 0.5577 µm + unidentified lines
2	3	0.589 - 0.770	Na I D + other lines from alkali metals
3	23	0.389 - 0.845	red O I at 0.6300 µm + other thermospheric lines
4	1	0.467 - 0.467	OH(7-0)
5	8	0.491 - 0.495	OH(8-1)
6	22	0.519 - 0.536	OH(9-2)
7	12	0.526 - 0.535	OH(6-0)
8	23	0.554 - 0.570	OH(7-1)
9	41	0.587 - 0.634	OH(8-2)
10	49	0.624 - 0.655	OH(9-3)
11	2	0.672 - 0.674	OH(10-4)
12	27	0.614 - 0.695	OH(5-0)
13	83	0.647 - 0.754	OH(6-1)
14	113	0.681 - 0.782	OH(7-2)
15	111	0.720 - 0.815	OH(8-3)
16	72	0.768 - 0.822	OH(9-4)
17	7	0.827 - 0.839	OH(10-5)
18	85	0.745 - 0.910	OH(4-0)
19	113	0.781 - 0.914	OH(5-1)
20	111	0.826 - 0.916	OH(6-2)
21	110	0.873 - 0.937	OH(7-3)
22	116	0.931 - 1.007	OH(8-4)
23	120	0.994 - 1.081	OH(9-5)
24	100	0.965 - 1.043	OH(3-0)
25	110	1.015 - 1.098	OH(4-1)
26	112	1.069 - 1.168	OH(5-2)
27	118	1.129 - 1.236	OH(6-3)
28	120	1.197 - 1.314	OH(7-4)
29	124	1.275 - 1.420	OH(8-5)
30	128	1.366 - 1.531	OH(9-6)
31	112	1.392 - 1.558	OH(2-0)
32	118	1.461 - 1.654	OH(3-1)
33	122	1.537 - 1.743	OH(4-2)
34	122	1.622 - 1.842	OH(5-3)
35	124	1.717 - 1.978	OH(6-4)
36	126	1.825 - 2.110	OH(7-5)
37	130	1.951 - 2.265	OH(8-6)
38	130	2.101 - 2.454	OH(9-7)
39	450	0.314 - 0.532	O_2(A-X) (Herzberg I)
40	5	0.324 - 0.410	O_2(c-X) (Herzberg II)
41	396	0.326 - 0.550	O_2(A'-a) (Chamberlain)
42	65	0.382 - 0.509	O_2(c-b)
43	208	0.656 - 0.806	O_2(b-X) (v' > v")
44	194	0.761 - 0.816	O_2(b-X) (v' = v")
45	103	0.861 - 0.922	O_2(b-X) (v' < v"; atmospheric 0-1 band inclusive)
46	161	1.240 - 1.305	O_2(a-X)(0-0) (IR atmospheric system)
47	73	1.555 - 1.598	O_2(a-X)(0-1) (IR atmospheric system)

Table 2: Description of B groups in the input line list

ID	Molecule	Upper state(s)	Remarks[a]
1	OH	$X^2\Pi_{1/2}, J' = 1/2$	Q2(0.5), P2(1.5)
2	OH	$X^2\Pi_{3/2}, J' = 3/2$	Q1(1.5), P1(2.5)
3	OH	$X^2\Pi_{1/2}, J' = 3/2$	R2(0.5), Q2(1.5), P2(2.5)
4	OH	$X^2\Pi_{3/2}, J' = 5/2$	R1(1.5), Q1(2.5), P1(3.5)
5	OH	$X^2\Pi_{1/2}, J' = 5/2$	R2(1.5), Q2(2.5), P2(3.5)
6	OH	$X^2\Pi_{3/2}, J' = 7/2$	R1(2.5), Q1(3.5), P1(4.5)
7	OH	$X^2\Pi_{1/2}, J' = 7/2$	R2(2.5), Q2(3.5), P2(4.5)
8	OH	$X^2\Pi_{3/2}, J' = 9/2$	R1(3.5), Q1(4.5), P1(5.5)
9	OH	$X^2\Pi_{1/2}, J' = 9/2$	R2(3.5), Q2(4.5), P2(5.5)
10	OH	$X^2\Pi_{3/2}, J' = 11/2$	R1(4.5), Q1(5.5), P1(6.5)
11	O_2	$b^1\Sigma_g^+, J' = 0, 2, 4$	
12	O_2	$b^1\Sigma_g^+, J' = 6, 8$	
13	O_2	$b^1\Sigma_g^+, J' = 10, 12$	
14	O_2	$b^1\Sigma_g^+, J' = 14, 16$	
15	O_2	$a^1\Delta_g, J' = 2, 4$	$v'' = 0$
16	O_2	$a^1\Delta_g, J' = 6, 8$	$v'' = 0$
17	O_2	$a^1\Delta_g, J' = 10, 12$	$v'' = 0$
18	O_2	$a^1\Delta_g, J' = 14, 16$	$v'' = 0$
19	O_2	$a^1\Delta_g, J' = 18, 20$	$v'' = 0$
20	O_2	$a^1\Delta_g, J' = 20, 22$	$v'' = 0$
21	O_2	$a^1\Delta_g, J' = 2, 4$	$v'' \neq 0$
22	O_2	$a^1\Delta_g, J' = 6, 8$	$v'' \neq 0$
23	O_2	$a^1\Delta_g, J' = 10, 12$	$v'' \neq 0$
24	O_2	$a^1\Delta_g, J' = 14, 16$	$v'' \neq 0$

[a] OH rotational transitions or lower vibrational level for O_2(a-X) transitions

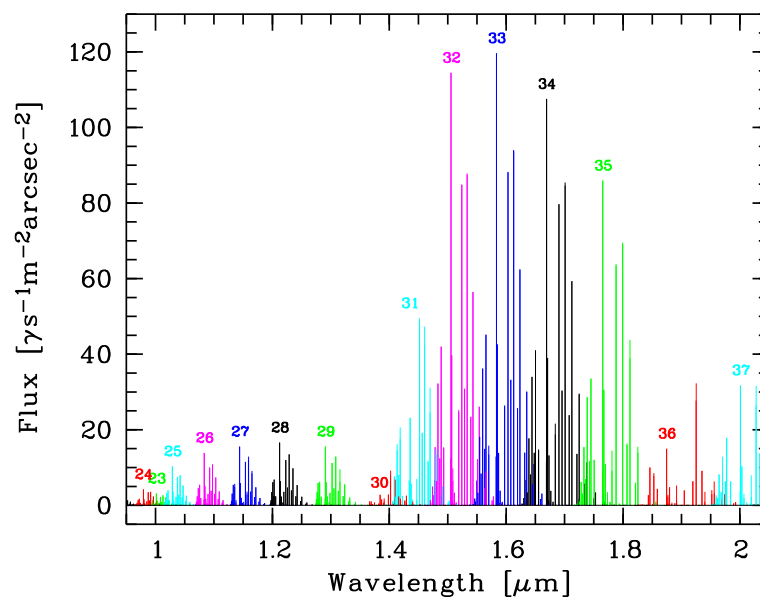Figure 13: A group identifications of the OH bands (cf. Table 1) in the wavelength range between 0.95 and 2.05 µm. The wavelengths and zenithal mean fluxes tabulated in the input line list are plotted.
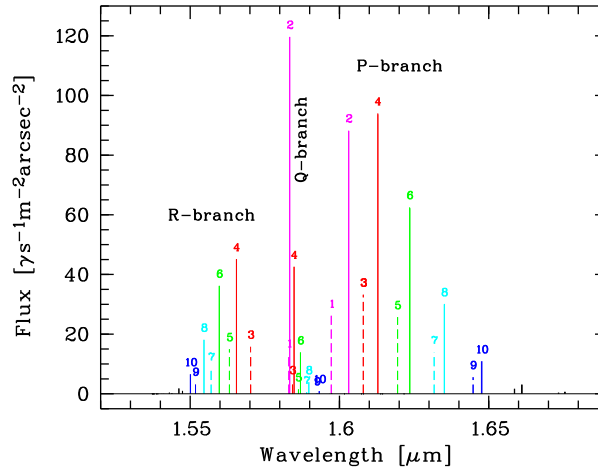
Figure 14: B group identifications of the transitions of an OH band with the same rotational upper state (cf. Table 2). The tabulated wavelengths and zenithal mean fluxes of the lines of the OH(6-4) band are shown as example. Dashed and solid lines indicate transitions of the $X^2\Pi_{1/2}$ and $X^2\Pi_{3/2}$ state, respectively. The figure also indicates the R-, Q-, and P-branches that correspond to transitions with a change of the total angular momentum by -1, 0, and 1, respectively.
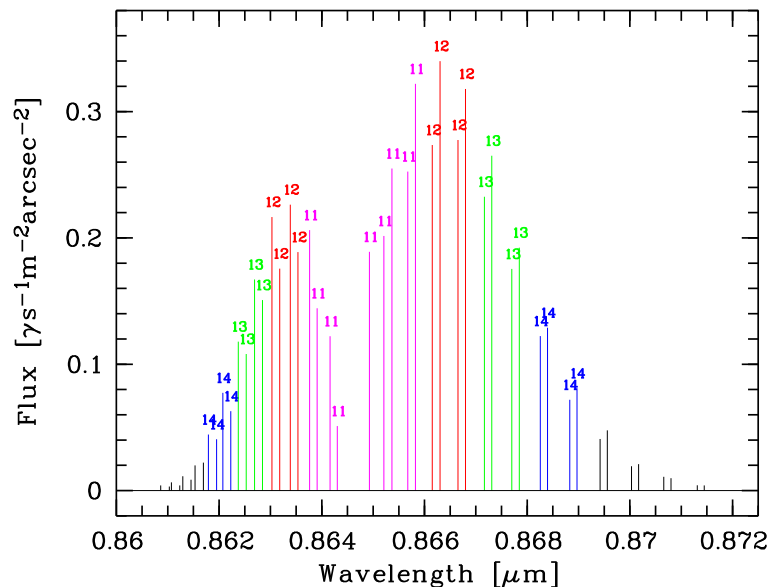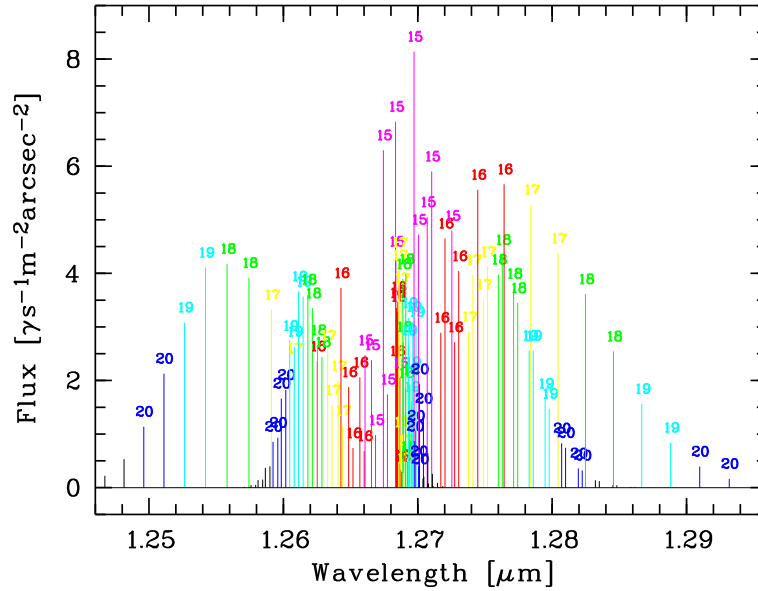

Figure 15: B group identifications of the transitions of the band O_2(b-X)(0-1) with a similar rotational upper state (cf. Table 2). The tabulated wavelengths and zenithal mean fluxes of the lines of the 4 different branches (2 R- and 2 P-branches) are shown (cf. Figure 14).

Figure 16: B group identifications of the transitions of the band $O_2(a-X)(0-0)$ with a similar rotational upper state (cf. Table 2). The tabulated wavelengths and zenithal mean fluxes of the lines of the 9 different branches (3 R-, 3 Q-, and 3 P-branches) are shown (cf. Figure 14). The band is strongly affected by self absorption in the lower atmosphere.
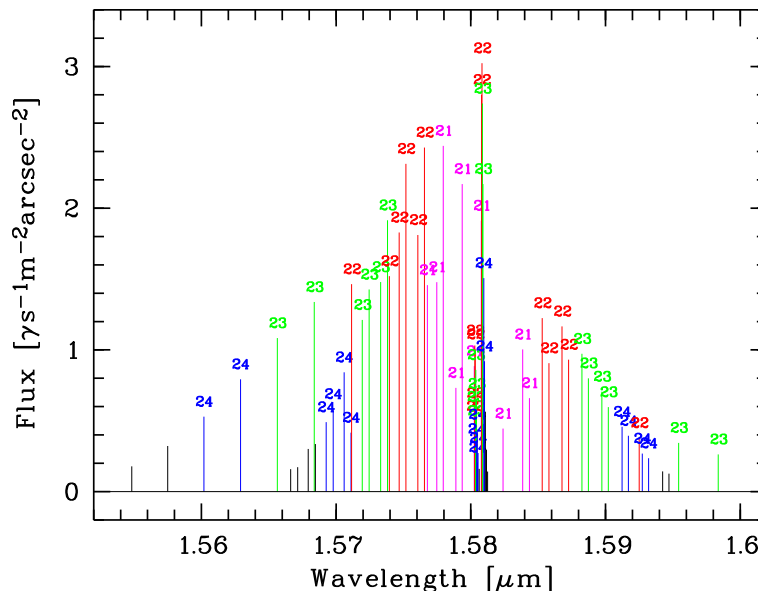

Figure 17: B group identifications of the transitions of the band $O_2(a-X)(0-1)$ with a similar rotational upper state (cf. Table 2). The tabulated wavelengths and zenithal mean fluxes of the lines of the 9 different branches (3 R-, 3 Q-, and 3 P-branches) are shown (cf. Figure 14).

5.4 Airglow model

The wavelength range from the near-UV to the near-IR is characterised by strong emission lines. Most of them constitute band structures. This airglow (see Khomich et al. [2008] for a comprehensive discussion) mostly originates in the mesopause region at about 90 km. In addition, some lines arise in the ionospheric F2-layer at about 270 km. In general, airglow is caused by chemiluminescence, *i.e.* chemical reactions that lead to light emission by the decay of excited electronic states of reaction products. Apart from atomic oxygen and sodium, the oxygen (O_2) and hydroxyl (OH) molecules are the most important reaction products in this context. In general, airglow lines show strong variability from time scales in the order of minutes to years. This behaviour can be explained by the solar activity cycle, seasonal changes in temperature, pressure, and chemical composition of the emission layers, the day-night contrast, dynamical effects such as gravity waves, or geomagnetic disturbances.

The SKYCORR project aims at correcting airglow emission in science spectra by means of reference sky spectra taken at a different time. As the airglow is highly variable, the strength of the emission lines in a reference spectrum has to be adapted, though. This is achieved by a fitting procedure that is discussed in Section 5.5. Since emission lines belonging to the science target should not be reproduced by the optimised sky spectrum and finally removed, it is advisable to adapt as many lines as possible by a single fitting parameter. Every group should contain airglow lines that are not affected by object lines and that can be used to determine a realistic correction factor for the reference sky spectrum. The number of lines that can be combined is limited by the fact that they should show an almost identical variability behaviour.

As basis for the definition of suitable line groups, the airglow line model developed in the course of the SM-01 project for an advanced sky background model for European Southern Observatory (ESO) exposure time calculators was used (see [SM-01] User Manual; Noll et al. [2012]). This semi-empirical model consists of a line list with line intensities for mean observing conditions and prescriptions for the correction of the line strength depending on molecular species, solar activity, season, night time, and zenith distance of the target. The latter three input parameters can be retrieved from the FITS header of the sky spectrum file. The solar activity is provided as solar radio flux at 10.7 cm either directly by SOLFLUX in the parameter file or by the corresponding monthly average (default) in a file offered by www.spaceweather.gc.ca (see Section 4.2). In the wavelength range from 0.3143 to 0.9228 μm, the line list consists of data taken from Cosby et al. [2006] (supplemented by unpublished UVES 800U data) who incorporated the UVES-based sky emission line atlas of Hanuschik [2003]. At longer wavelengths the calculated OH lines of Rousselot et al. [2000] were included. However, their line strengths were corrected for the Einstein factors of Goldman et al. [1998] instead of using the original, outdated ones of Mies [1974]. This resulted in correction factors for OH band strengths between 0.38 and 2.06. Moreover, the flux decrease of airglow lines by molecular absorption in the lower atmosphere was corrected by the multiplication of the airglow line spectrum with Doppler line widths for typical temperatures of about 200 K by the high-resolution ($\lambda/\Delta\lambda \approx 10^6$) Paranal annual-mean transmission curve for an airmass of 1.25^5 (see Noll et al. [2012]). The transmission curve was computed by means of the radiative transfer code

---

[4]Note that this component is very difficult to determine. Its measured intensity strongly depends on the accuracy of the other components, the quality of the flux calibration, and possible instrumental continua. For this reason, it should also been seen as residual continuum.

[5]Although the atmospheric transmission depends on airmass and weather conditions, only a fixed airglow flux correction was applied in order to avoid time-consuming calculations at very high resolution and the input of temperature and water vapour profiles. Moreover, the optical airglow atlas of Hanuschik [2003] is also characterised by a fixed transmission correction due to the use of UVES mean spectra. For most observing conditions, the deviation of the true airglow absorption from the assumed one is expected to be minor in terms of the results of SKYCORR.

LBLRTM (see Clough et al. [2005] and [6]). Note that SKYCORR applies the Paranal mean transmission curve for zenith (corrected for the target airmass) to the unextincted fluxes in the input line list. For this purpose, the line list contains separate columns for unextincted line fluxes and zenithal transmission values. Finally, the Rousselot et al. lines were scaled to the Cosby et al. lines between 0.642 and 0.858 μm. The strongest O_2 bands in the near-IR at 1.27 and 1.58 μm were included in the line list by adding data from the HITRAN database (see Rothman et al. [2009] and [3]). The mean band strength was roughly estimated evaluating the ratio of O_2 to OH lines in 26 IR X-Shooter spectra. For this purpose, the O_2 lines had to be extincted depending on the airmass values of the X-Shooter spectra. In the case of the 1.27 μm band, this caused significant changes in the line fluxes due to the strong resonant absorption of airglow photons by tropospheric/stratospheric O_2 molecules in the ground state.

The SM-01 sky model assigns the listed lines to five different variability classes (see Figure 10). These variability classes result from analysing a sample of 1189 optical FORS spectra (Patat [2008]). From this sample, the lines' dependence on solar radio flux and time of observation (see Figure 11) was derived. The latter was quantified using a grid of six double month periods starting with Dec/Jan and three night time bins of equal length. The reference line strengths in the line list represent the mean of the five solar activity cycles 19 to 23, *i.e.* the years 1954 to 2007.

Assigning airglow lines to the classes (1) green O I, (2) Na I D, (3) red O I, (4) OH, and (5) O_2 using the rough predictions from the sky model is not sufficient for achieving a line intensity accuracy on the percent level and better, which is required for a sky subtraction procedure like SKYCORR. Typically, intensity variations of lines within a variability class are larger. The ratios of line strengths of different variability classes vary by a factor of two or even more.

In principle, an identical variability behaviour can be expected for transitions with the same upper energy level. In this case, the ratios of line intensities should be fixed and only determined by quantities such as Einstein coefficients and statistical weights. On the other hand, the excitation and population of different energy levels depends on variable quantities such as temperature, pressure, and chemical abundances. Therefore, it is a promising ansatz to define line groups depending on the upper energy level. However, taking all relevant energy levels of the molecules OH and O_2 into account would result in a very large number of line groups. Moreover, each group would consist of only a few significant lines. This would result in statistical fluctuations, which could make the line intensity correction uncertain if crucial lines of a group were affected by, *e.g.*, CCD defects or object emission lines (see Section 5.5). Fortunately, as their energies are rather different, it is possible to separate electronic, vibrational, and rotational transitions of molecules. The electronic/vibrational transition determines the band and the rotational transition identifies a single line or doublet (as in case of OH) within a band. Since the distribution of energy levels is very similar for all bands of an electronic transition, each line can be assigned to two different classes that are defined by the upper vibrational and rotational state. This approach reduces the number of required line groups significantly. Moreover, for OH only the electronic ground state is relevant, which splits up into the sub-levels $X^2\Pi_{1/2}$ and $X^2\Pi_{3/2}$ due to the coupling of spin and orbital angular momentum (see Rousselot et al. [2000]). For O_2, the electronic transitions are more important than the vibrational ones, since the intensity differences of the bands of an electronic transition are very large. Consequently, there are only three O_2 bands that significantly contribute to the airglow, namely O_2(b-X)(0-1)[6] (the very strong (0-0) band is almost completely absorbed in the lower atmosphere), O_2(a-X)(0-0), and O_2(a-X)(0-1).

---

[6]The notation used is as follows: molecule (upper - lower electronic state) (upper - lower vibrational state). The letters 'a', 'b', and 'X' are shortcuts for the states $a^1\Delta_g$, $b^1\Sigma_g^+$, and $X^3\Sigma_g^-$. The vibrational states are numbered depending on the energy and starting from 0 for the lowest level.

		Doc:	VLT–MAN–ESO–19550–5896
ESO	SKYCORR sky correction:	Issue:	Issue 4.4
	User documentation and evaluation	Date:	Date 2014–04–01
		Page:	45 of 70

Tables 1 and 2 list the final grouping of airglow lines. Line groups with the same upper electronic/vibrational level are called "A groups" and those with the same (OH) or a similar (O_2) upper rotational level are labelled as "B groups". Most OH bands (apart from a few very weak ones) are identified in the Figures 12 and 13. Although bands such as OH(4-1) and OH(4-2) have the same upper vibrational level, they represent independent variability groups. Although significantly increasing the number of A groups, the fact that real data suffer from calibration uncertainties, makes this procedure a necessity. As OH bands with the same upper vibrational level are widely separated, it is therefore safer to vary such bands independently. Figures 14, 15, 16, and 17 show identifications of the rotational B groups for an example OH band, O_2(b-X)(0-1), O_2(a-X)(0-0), and O_2(a-X)(0-1), respectively. Although the two O_2(a-X) bands belong to the same roto-vibrational system, their B groups were defined separately due to the completely different line flux distribution which is caused by self absorption in the (0-0) band. B groups of O_2 bands consist of lines from two rotational upper levels in order to make sure that enough lines can be identified for the group scaling (see Section 5.5). The weak lines of each band are not included in a B group as they are difficult to fit. Furthermore, this measure avoids a degeneration of fit parameters.

The described grouping is reminiscent of the approach of Davies [2007]. However, it is much more complex, since Davies only incorporates near-IR OH bands, O_2(a-X)(0-0), and two rotational groups resembling our B 2 and B 4 classes (see Table 2).

5.5   Airglow line fitter

To prepare a reference sky line spectrum taken at a different time than the corresponding science spectrum for a background subtraction, this reference spectrum has to be adapted. To this end, Davies [2007] sub-divides the wavelength range into sections depending on the OH band structure and subsequently scales these sections independently according to the sections' flux ratio of science and sky spectra. Problematic are cases where different line groups have significant overlap. While the OH bands covered in SINFONI *H*-band spectra exhibit only little overlap and no significant band of other molecules are present, at lower wavelengths the situation is less favourable (see Section 5.4). Even so, measuring the scaling factors for groups with the same upper rotational level is difficult. Here, the flux of individual lines has to be derived, which requires that the selected lines are isolated. Typically, this is not the case for Q transitions, which are characterised by a constant total angular momentum (see Figure 14). Furthermore, the separation of variability groups becomes even more difficult if the spectral resolution is relatively low as in the case of the FORS spectra shown in Figure 10.

To overcome these limitations, the SKYCORR project pursues a completely different approach to obtaining the scaling factors for the different line groups defined in Section 5.4. In SKYCORR, the contributions of the line groups to each pixel of the sky spectrum are estimated. Subsequently, the resulting spectra for each line class ($\leq 100\%$ of the total sky flux) are scaled.

This is performed applying the airglow model presented in the previous section. The wavelengths and intensities of the lines and their group identifications can be converted into intensities of the different line groups for each pixel. This requires a convolution of the lines from the line list with a kernel similar to the instrumental profile of the observed spectra. The mean FWHM of the sky lines, which was obtained in a previous step (see Section 5.2), is used for creating a sufficently realistic Gaussian kernel. In order to treat intensity ratios of overlapping lines as realistically as possible, the airglow variability model from Noll et al. [2012] (see Section 5.4) was included. This allows one to rougly correct for the influence of solar activity, season, and night time on the main line variability classes green O I, Na I D, red O I, OH, and O_2.

		Doc:	VLT–MAN–ESO–19550–5896
ESO	SKYCORR sky correction:	Issue:	Issue 4.4
	User documentation and evaluation	Date:	Date 2014–04–01
		Page:	46 of 70

Different line groups contributing to the same pixel implies that the sky scaling factors cannot be derived by a simple division of line fluxes of science and sky spectrum anymore. Instead, each scaling factor of the individual line groups has to be included in a fitting procedure as a free fitting parameter. For this purpose, the C library MPFIT by C. Markwardt [1] (see Section 5.2) was used. The χ^2 minimisation procedure of this routine is based on a Levenberg-Marquardt technique (see Moré et al. [1980]), an iterative search algorithm characterised by gradient-controlled jumps in parameter space. Since this technique is potentially prone to finding local minima, reasonable starting values and constraints for the fit parameters are required. For this reason, the mean ratios of the line peaks in the science and sky spectrum are calculated for each line group (see Section 5.4). Only those spectrum pixels are included that were identified as line peak (see Section 5.1) or are separated from a peak by not more than half a line FWHM (see Section 5.2) and have a relative contribution of the selected line group of at least WEIGHTLIM (default: 0.67; see Section 4.2). Moreover, pixels with unreasonable flux ratios are rejected by applying a global σ limit that is derived from the full set of line peaks and is provided by the parameter SIGLIM (default: 15; see Section 4.2). In this way, strong object emission lines can be identified in the science line spectrum and excluded. Finally, the σ-clipping approach with variable σ limit described in Section 5.2 is applied to the selected pixels of each group separately in order to further improve the pixel selection. The remaining pixels of this procedure are taken for the initial line group scaling *and* fitting algorithm, *i.e.* only those pixels are considered for the χ^2 calculation. If suitable pixels cannot be found for a line group, a mean flux ratio of the corresponding system of electronic transitions (*e.g.* OH; see Section 5.4) or a global flux ratio is taken for A groups and a value of 1 is assumed for B groups. For most sky spectra this approach should result in a good first guess sufficient for achieving rapid convergence to the global minimum (see Section 6).

As an option the fitting can be restricted to uncertain line groups only. The decision on the group selection depends on the parameter FITLIM (see Section 4.2) which provides a limiting ratio of the RMS and the mean of the group-specific scaling factors. By default this value is set to 0, *i.e.* all fittable line groups are considered.

5.6 Correction of wavelength grid

Since the sky lines of the science spectrum are removed by a scaled reference sky line spectrum, it is imperative that the wavelength grids of both spectra are aligned. Differences of less than a pixel can already significantly deteriorate the quality of the sky subtraction. Relatively large deviations can occur if a lamp spectrum taken in daytime at different ambient conditions than the science spectrum is used for the wavelength calibration. However, even subpixel shifts that are routinely observed in data taken under perfect conditions can cause problems.

For this reason, SKYCORR offers optional correction of the wavelength grid by applying a Chebyshev polynomial of degree n_{w}

$$\lambda' = \sum_{i=0}^{n_{\mathrm{w}}} c_i t_i, \tag{1}$$

where

$$t_i = \begin{cases} 1 & \text{for } i = 0 \\ \lambda & \text{for } i = 1 \\ 2\,\lambda\,t_{i-1} - t_{i-2} & \text{for } i \geq 2 \end{cases} \tag{2}$$

and λ ranging from -1 to 1. The temporary conversion of the wavelength grid to a fixed interval results in coefficients c_i independent of the wavelength range and step size of the input spectrum. The wavelength solution is not changed if $c_1 = 1$ and $c_i = 0$ for all other i. It is possible to set an individual start value for the constant

		Doc:	VLT–MAN–ESO–19550–5896
ESO	SKYCORR sky correction:	Issue:	Issue 4.4
	User documentation and evaluation	Date:	Date 2014–04–01
		Page:	47 of 70

term c_0 via the parameter CHEBY_CONST (see Section 4.2). In this way, significant possible shifts between the wavelength grids of the science and the sky spectrum can be considered.

The coefficients c_i are determined by an iterative procedure. This process is initialised with two subsequent estimates (for a better σ-clipping) and a fit of the line flux correction factors (see Section 5.5). During this first iteration the wavelength grid remains untouched. In the next step, the coefficients c_0 and c_1 are fitted using MPFIT. Now, a new estimate is calculated and the line flux correction factors are fitted again. Then the next iteration starts by fitting the wavelength grid, now applying a Chebyshev polynomial of degree 2. After that, the line scaling factors are adapted again in order to incorporate the change of the wavelength grid. Each iteration increases n_w by 1 and uses the results of the previous iteration as input. The search for the best polynomial degree is controlled by the three input parameters CHEBY_MIN, CHEBY_MAX, and WTOL (see Section 4.2). The iteration process is stopped once the maximum polynomial degree given by CHEBY_MAX is reached. For a value of -1, no wavelength grid correction is performed. The parameter CHEBY_MIN indicates the minimum degree, *i.e.* the minimum number of iterations. For n_w not less than CHEBY_MIN, the code checks whether the resulting χ^2 shows a relative χ^2 improvement of at least WTOL (default: 1×10^{-3}) compared to the best χ^2, so far. If this is not the case the procedure stops and the results for the polynomial with the lowest χ^2 are taken. An exception is a choice of CHEBY_MIN > CHEBY_MAX. In this case, the code runs until CHEBY_MAX is reached and the corresponding results for this degree are taken, regardless of the results for the lower polynomial degrees. The default values for CHEBY_MAX and CHEBY_MIN are 7 and 3, respectively.

Independent of the use of a Chebyshev polynomial, the modified sky spectrum has to be rebinned to the wavelength grid of the science spectrum. For this task, the code offers two options, which can be selected by the parameter REBINTYPE (see Section 4.2). The first method adds up the fractional fluxes of input pixels contributing to the wavelength range of the output pixel. The second approach is based on the convolution of the input spectrum with a pixel-dependent asymmetric damped sinc kernel

$$f(k) = e^{-((k-s)/\delta)^2} \frac{\sin(\pi(k-s))}{\pi(k-s)}, \tag{3}$$

with k being an integer variable ranging from $-k_{max}$ to k_{max}. The damping constant δ and the kernel radius k_{max} are fixed and have the values 3.25 and 5. The parameter s is the subpixel shift of the sky spectrum relative to the science spectrum. It is a function of the pixel position and ranges from -0.5 to 0.5. For shifts above half a pixel, complete pixels are treated by a simple renumbering of the input pixels in the output spectrum. No convolution is performed for this integer part of the pixel shift. The approach is similar to the one used in the IDL routine "sshift2d.pro" of the Lowell Buie Library [4]. However, the original programme is for a constant shift of the entire spectrum only. A wavelength-dependent shift is not a problem as long as the amount of the shift changes slowly with the spectrum pixels and the pixel size is nearly constant for the whole input and output wavelength grids. These requirements are sufficiently met if inconsistencies of the wavelength grids are in the order of 1 pixel and if the functional dependence of differences can be described by a low order polynomial. The relatively complicate rebinning method described above is able to effectively suppress broadening of spectral lines, which typically occurs if a spectrum is rebinned to a shifted grid of similar pixel size. The line-broadening suppression is achieved by alternating positive and negative contributions to the kernel as incorporated in the sinc shift method. Therefore, the sinc shift method produces the best results if significant subpixel shifts close to half a pixel are frequent. However, for a very good agreement of the wavelength grids with subpixel shifts close to zero, it might be better to use the simple rebinning method. In such a case, the relatively broad sinc kernel influences the spectrum more than simple regridding.

Table 3: Description of test sky spectra

label	Instrument	Resol.[a]	λ range [μm]	Date	Time [UT]	$S_{10.7\,cm}$[b] [sfu]	Elevation [deg]
fors_0114	FORS 1	1200	0.54 − 0.75	2000-06-25	01:23	180	54.6
fors_0150	FORS 1	500	0.36 − 0.89	2000-08-26	05:48	164	70.7
fors_0918	FORS 1	500	0.36 − 0.89	2004-02-26	06:23	107	67.7
fors_0919	FORS 1	500	0.36 − 0.89	2004-02-26	06:59	107	74.3
fors_1153	FORS 1	1200	0.54 − 0.75	2004-11-18	07:05	116	55.7
fors_1154	FORS 1	1200	0.54 − 0.75	2004-11-18	08:08	116	46.3
sinfo_1	SINFONI	2700	1.44 − 1.83	2005-04-03	00:00	86	50.6
sinfo_2	SINFONI	2700	1.44 − 1.83	2005-04-03	06:32	86	75.8
sinfo_4	SINFONI	3400	1.94 − 2.45	2005-04-03	10:05	86	57.1
sinfo_5	SINFONI	3400	1.94 − 2.45	2005-08-11	00:54	98	60.6
sinfo_6	SINFONI	2000	1.10 − 1.36	2005-10-31	00:34	77	51.7
sinfo_7	SINFONI	2000	1.10 − 1.36	2006-03-13	06:05	76	68.4
xshoo_28	X-Shooter	5300	0.99 − 2.00	2010-03-05	02:02	83	55.8
xshoo_29	X-Shooter	5300	0.99 − 2.00	2010-03-06	00:52	83	57.2
xshoo_39	X-Shooter	3200	0.99 − 2.00	2010-03-22	04:04	83	64.9
xshoo_42	X-Shooter	5300	0.99 − 2.00	2010-03-29	05:38	83	56.9
xshoo_43	X-Shooter	3200	0.99 − 2.00	2010-04-19	00:07	76	42.8
xshoo_44	X-Shooter	3200	0.99 − 2.00	2010-04-19	01:59	76	62.9

[a] mean wavelength / line FWHM

[b] monthly average of solar radio flux at 10.7 cm in s.f.u. (= 0.01 MJy)

6 Validation

The performance of SKYCORR is discussed in the following. Section 6.1 describes the test set-up. The results are discussed in Section 6.2. Finally, SKYCORR is compared to the SINFONI pipeline procedure based on the Davies method (Section 6.3). Some test data are available in the code directory `<INST_DIR>/examples/` (see Section 4.6). This folder also contains a set of X-Shooter spectra, which is extensively discussed in the project's science report [SM-03-SR].

6.1 Test set-up

SKYCORR was applied to sky spectra taken from the sky model verification data set (see [SM-01] User Manual). Spectra from the FORS 1, SINFONI, and X-Shooter instruments were used (see Tables 3 and 4). Davies' [2007] method was developed for SINFONI IR spectra. The present SINFONI data set comprises two *J*-band, two *H*-band, and three *K*-band spectra. With these data a single test per band was performed, using one spectrum as input science spectrum and one as reference sky spectrum. The available SINFONI spectra are challenging for the sky subtraction procedure, since the spectra of each band show exceptionally pronounced differences (see [SM-01] User Manual). In addition, the *J*-band spectra were taken about half a year apart. In order to

Table 4: Test results for pure sky spectra

Target sky	Ref. sky	N_A[a]	c_A[b]	N_B[a]	c_B[b]	N_w[a]	$\frac{\sigma(\Delta f_{peak})}{\langle f_{peak}\rangle}$[c] [%]	$\langle\frac{\Delta f_{peak}}{f_{peak}}\rangle$[d] [%]	t_{fit}[e] [s]	t_{code}[e] [s]
fors_0918	fors_0919	13	1.00 – 1.21	10	0.98 – 1.01	6	0.3	0.3	5.1	8.7
fors_0150	fors_0919	13	0.82 – 1.47	10	0.95 – 1.05	4	2.5	1.9	6.0	10.0
fors_1153	fors_1154	9	0.86 – 1.00	10	0.98 – 1.00	2	0.9	0.9	2.3	5.1
fors_0114	fors_1154	9	0.70 – 2.56	10	0.52 – 0.61	8	8.6	4.3	17.6	20.0
sinfo_1	sinfo_2	6	1.84 – 4.26	14	1.12 – 2.46	4	3.0	2.7	8.8	10.3
sinfo_4	sinfo_5	3	1.25 – 1.49	10	0.84 – 0.98	2	3.7	3.3	2.1	3.6
sinfo_6	sinfo_7	5	2.00 – 5.93	16	0.88 – 1.80	4	3.6	2.9	4.4	5.9
xshoo_28	xshoo_29	17	0.37 – 0.72	20	0.93 – 1.21	5	7.3	5.8	57.3	75.8
xshoo_42	xshoo_29	17	0.18 – 0.95	20	0.52 – 1.81	3	6.5	6.9	44.4	62.4
xshoo_43	xshoo_44	17	0.82 – 1.80	20	0.71 – 1.51	0	3.0	3.1	44.8	67.3
xshoo_39	xshoo_44	17	0.37 – 1.46	20	0.89 – 1.69	3	3.7	3.6	48.7	68.0

[a] number of fitted A groups, B groups, and coefficients for polynomial wavelength grid correction

[b] range of line flux scaling factors for fitted A and B groups

[c] RMS from difference between modified sky line peaks and input science line peaks relative to mean of science line peaks (flag $\geq$ 2; see Section 5.1). The values can be higher if unclipped object emission lines contribute to the RMS measurement (see Section 5.5).

[d] σ-clipped mean ratio of sky correction residual and line flux for line peaks

[e] tested on a Core2Quad Q9550@2.83GHz, 8GB RAM, Fedora 16 (64 bit)

Table 5: Test results for object spectra

Object[a]	Object sky	Ref. sky	N_A[b]	c_A[c]	N_B[b]	c_B[c]	N_w[b]	$\frac{\sigma(\Delta f_{peak})}{\langle f_{peak}\rangle}$[d] [%]	$\langle\frac{\Delta f_{peak}}{f_{peak}}\rangle$[e] [%]	t_{fit}[f] [s]	t_{code}[f] [s]
NGC 4594	fors_0918	fors_0919	13	0.88 – 2.78	10	0.61 – 0.97	4	9.2	12.1	5.2	8.8
NGC 4625	fors_0918	fors_0919	12	0.29 – 1.58	10	0.81 – 1.44	0	21.6	18.8	11.0	14.9
NGC 4594	sinfo_1	sinfo_2	6	2.09 – 7.48	10	1.05 – 1.16	0	3.5	3.3	4.0	6.3
NGC 4625	sinfo_1	sinfo_2	6	1.93 – 7.73	10	1.14 – 1.27	3	3.4	2.9	2.4	4.6
NGC 4594	sinfo_6	sinfo_7	5	1.69 – 2.58	16	1.11 – 2.39	0	17.5	16.6	11.1	13.1
NGC 4625	sinfo_6	sinfo_7	5	1.92 – 2.93	16	1.08 – 2.23	0	23.2	16.2	6.3	8.0
NGC 4594	xshoo_28	xshoo_29	16	0.40 – 0.75	16	0.95 – 1.19	7	6.9	5.6	75.3	96.9
NGC 4625	xshoo_28	xshoo_29	16	0.41 – 0.75	16	0.86 – 1.10	5	6.6	5.5	54.2	76.1
NGC 4594	xshoo_43	xshoo_44	17	0.77 – 1.21	16	1.00 – 2.11	0	3.5	3.8	51.6	78.2
NGC 4625	xshoo_43	xshoo_44	17	0.61 – 2.16	10	0.97 – 1.10	0	3.5	3.8	26.1	48.8

[a] best-fit CIGALE spectrum of given galaxy at $z = 0.5$ with arbitrary scaling plus additional emission lines at 0.5, 0.61, 0.71, 0.799553, 0.843248, 1.12, 1.153871, 1.19, 1.212263, 1.34, 1.50, 1.60, 1.670881, 1.700843, and 1.77 μm depending on the wavelength range of the spectrum

[b] number of fitted A groups, B groups, and coefficients for polynomial wavelength grid correction

[c] range of line flux scaling factors for fitted A and B groups

[d] RMS from difference between modified sky line peaks and input science line peaks relative to mean of science line peaks (flag $\geq$ 2; see Section 5.1). The values can be higher if unclipped object emission lines contribute to the RMS measurement (see Section 5.5).

[e] σ-clipped mean ratio of sky correction residual and line flux for line peaks

[f] tested on a Core2Quad Q9550@2.83GHz, 8GB RAM, Fedora 16 (64 bit)
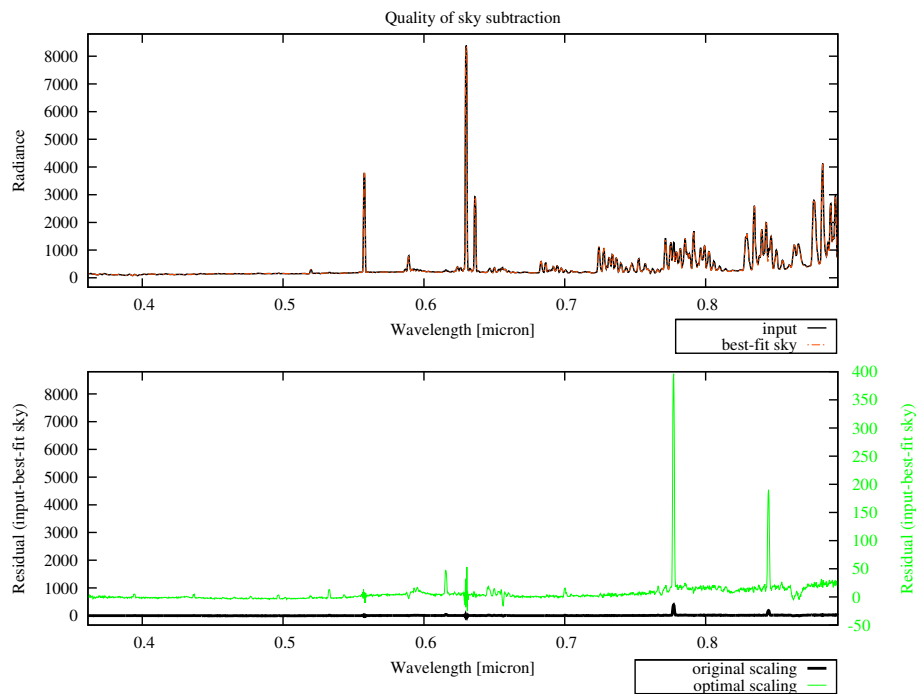
Figure 18: Comparison of fors_0918 (black) and best-fit fors_0919 (red). The upper panel shows the input and the best-fit spectra, the lower panel the residual in two different scalings (black = original scaling, green = optimal scaling).

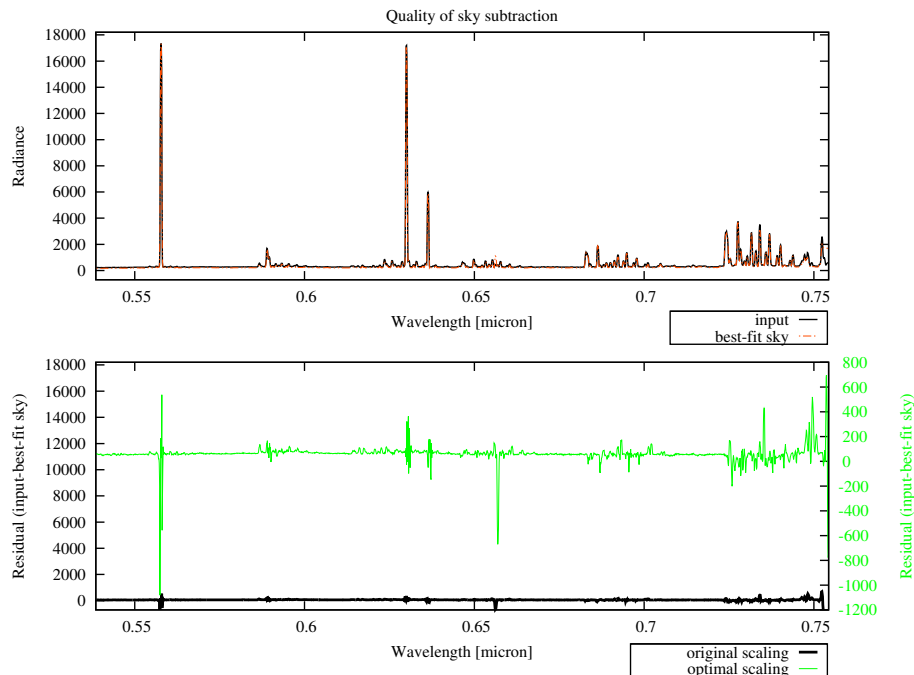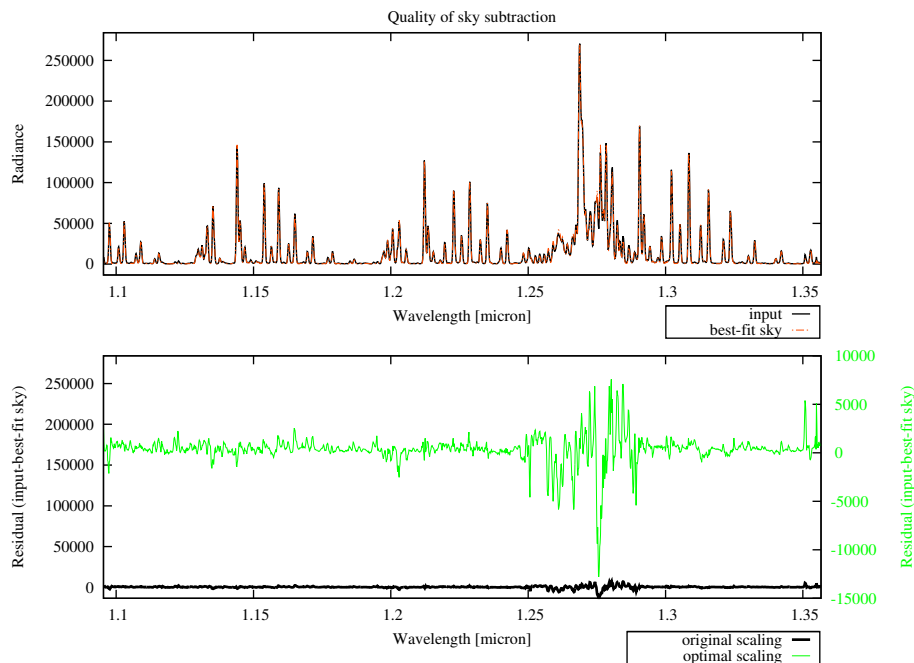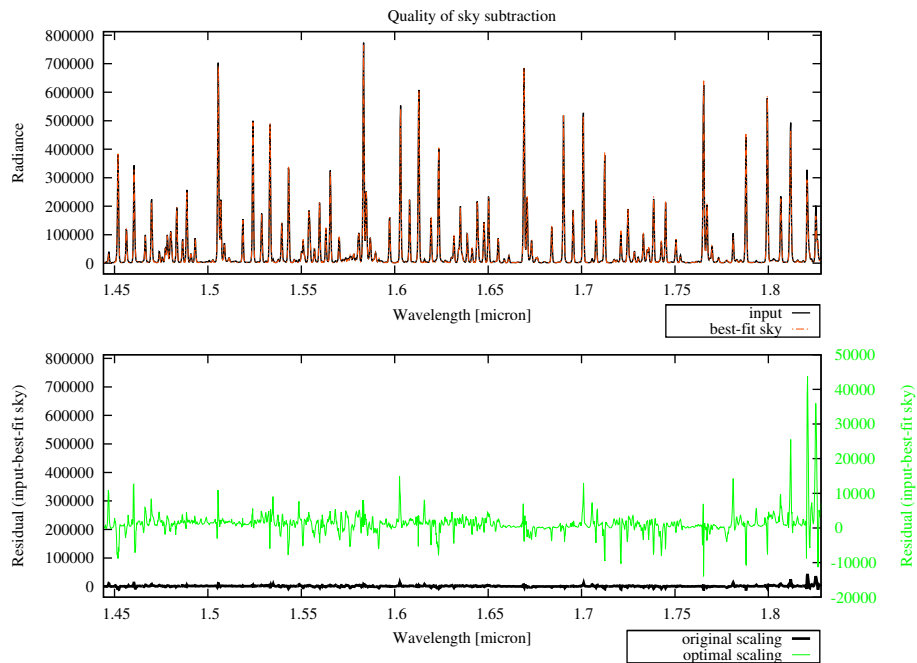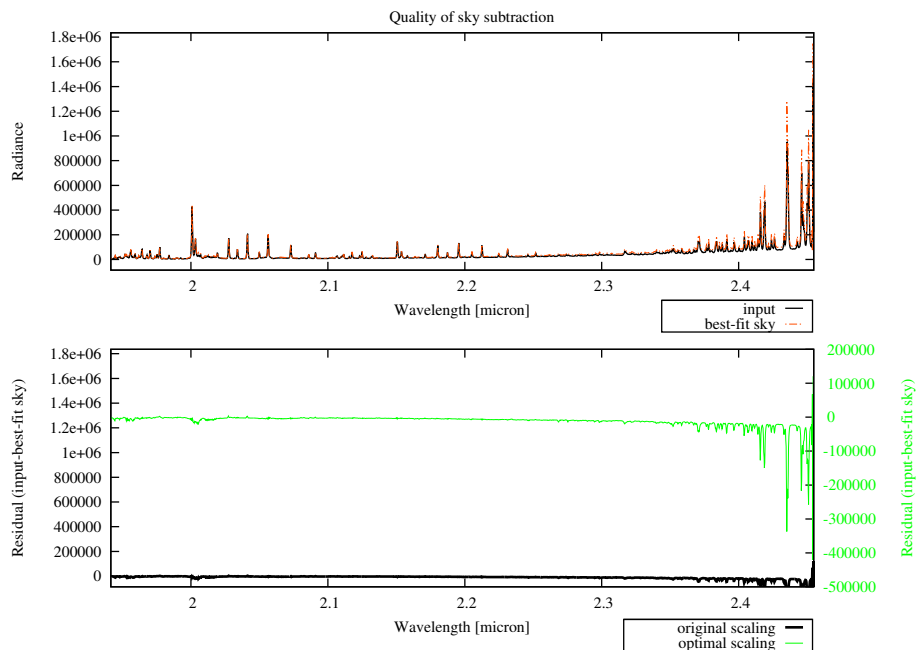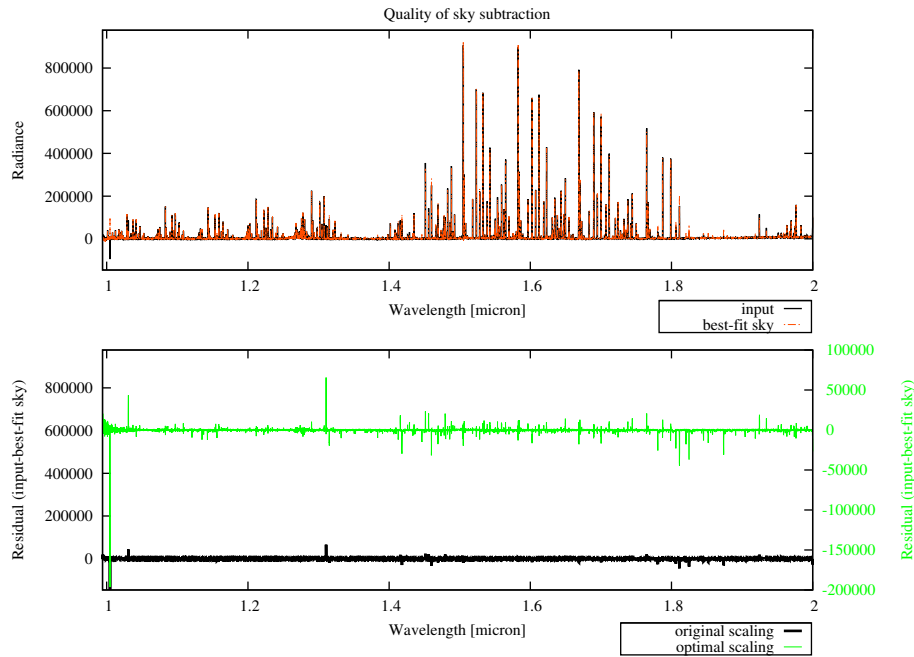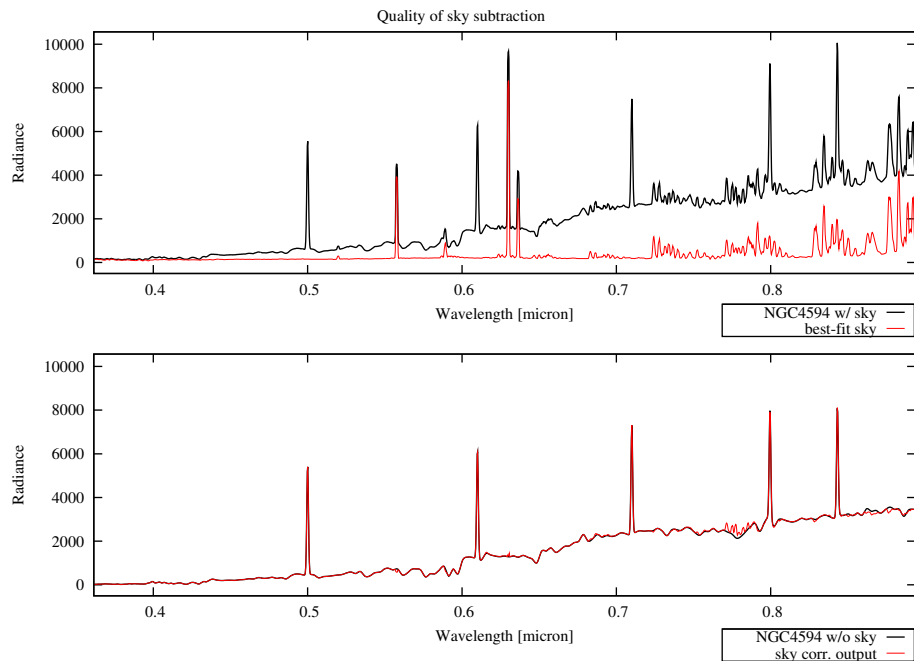Figure 19: Comparison of fors_0114 (black) and best-fit fors_1154 (red). The upper panel shows the input and the best-fit spectra, the lower panel the residual in two different scalings (black = original scaling, green = optimal scaling).

Figure 20: Comparison of sinfo_6 (black) and best-fit sinfo_7 (red). The upper panel shows the input and the best-fit spectra, the lower panel the residual in two different scalings (black = original scaling, green = optimal scaling).

Figure 21: Comparison of sinfo_1 (black) and best-fit sinfo_2 (red). The upper panel shows the input and the best-fit spectra, the lower panel the residual in two different scalings (black = original scaling, green = optimal scaling).

Figure 22: Comparison of sinfo_4 (black) and best-fit sinfo_5 (red). The upper panel shows the input and the best-fit spectra, the lower panel the residual in two different scalings (black = original scaling, green = optimal scaling).

Figure 23: Comparison of xshoo_28 (black) and best-fit xshoo_29 (red). The upper panel shows the input and the best-fit spectra, the lower panel the residual in two different scalings (black = original scaling, green = optimal scaling).

Figure 24: Comparison of arbitrarily scaled NGC 4594 spectrum at $z = 0.5$ + artificial emission lines of equal intensity at 0.5, 0.61, 0.71, 0.799553, 0.843248 μm + fors_0918 (black) and best-fit fors_0919 (red). The lower panel shows the sky subtraction residual (red) and the original, not sky-affected NGC 4594 spectrum (black).
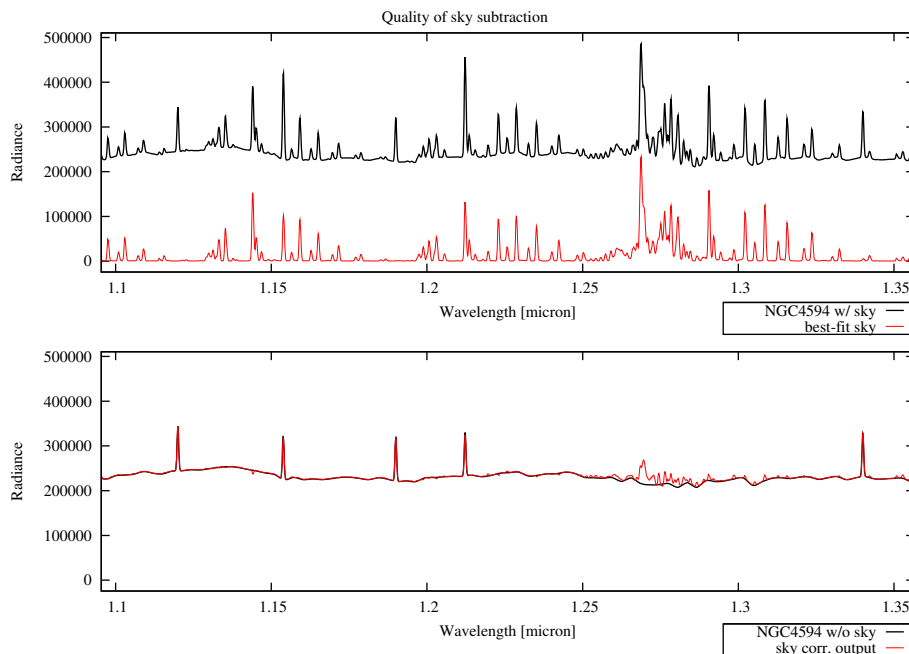
Figure 25: Comparison of arbitrarily scaled NGC 4625 spectrum at $z = 0.5$ + artificial emission lines of equal intensity at 0.5, 0.61, 0.71, 0.799553, 0.843248 μm + fors_0918 (black) and best-fit fors_0919 (red). The lower panel shows the sky subtraction residual (red) and the original, not sky-affected NGC 4625 spectrum (black).

Figure 26: Comparison of arbitrarily scaled NGC 4594 at $z = 0.5$ + artificial emission lines of equal intensity at 1.12, 1.153871, 1.19, 1.212263, and 1.34 μm + sinfo_6 (black) and best-fit sinfo_7 (red). The lower panel shows the sky subtraction residual (red) and the original, not sky-affected NGC 4594 spectrum (black).

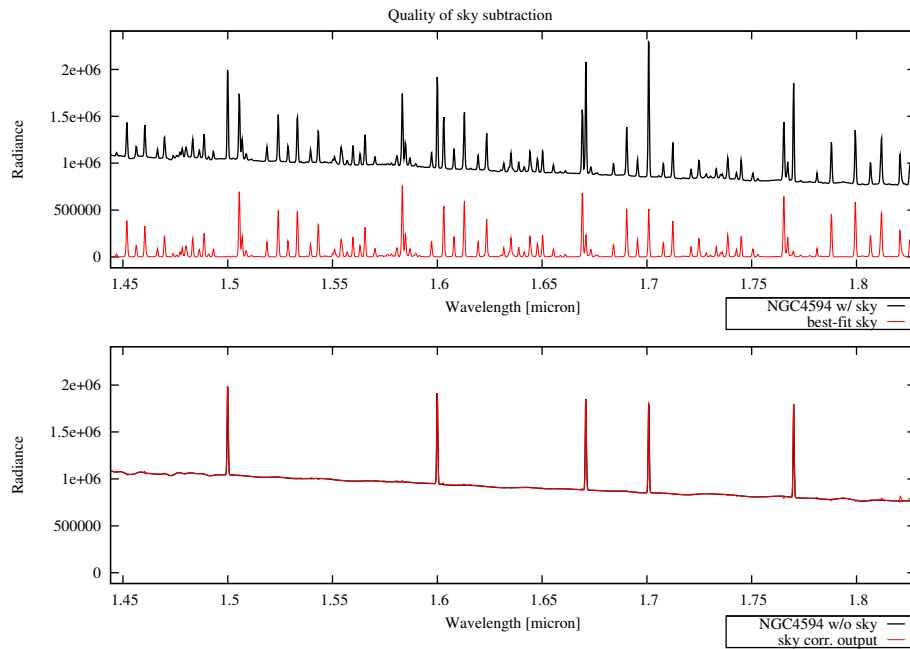|		Doc:	VLT–MAN–ESO–19550–5896
ESO	SKYCORR sky correction:	Issue:	Issue 4.4
	User documentation and evaluation	Date:	Date 2014–04–01
		Page:	56 of 70

Figure 27: Comparison of arbitrarily scaled NGC 4594 at $z = 0.5$ + artificial emission lines of equal intensity at 1.50, 1.60, 1.670881, 1.700843, and $1.77\,\mu$m + sinfo_1 (black) and best-fit sinfo_2 (red). The lower panel shows the sky subtraction residual (red) and the original, not sky-affected NGC 4594 spectrum (black).
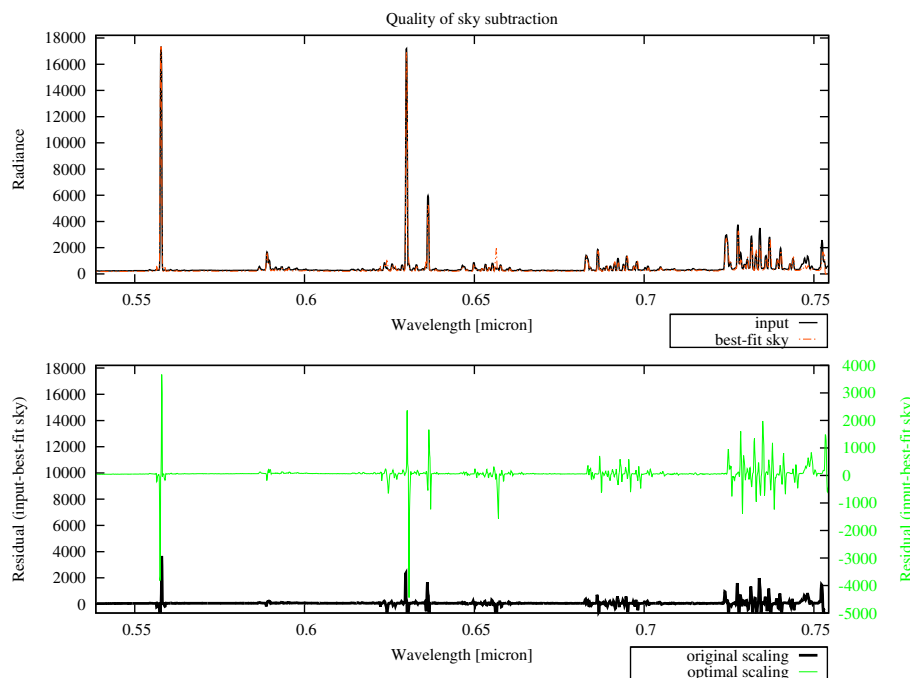
Figure 28: Comparison of fors_0114 (black) and best-fit fors_1154 (red) for no correction of the wavelength grid by the fit of a Chebyshev polynomial. The upper panel shows the input and the best-fit spectra, the lower panel the residual in two different scalings (black = original scaling, green = optimal scaling).

have more realistic input spectra, we also facilitate four pairs of X-Shooter NIR arm spectra obtained with 0.9″ and 1.5″ slits, respectively. The two combinations for each instrumental set-up differ in the time difference of both exposures. Short time periods are in the order of one hour or one night, while long time spreads are in the order of one month. For long time differences, the available sample of X-Shooter spectra in not suitable. Finally, we also tested four pairs of FORS 1 sky spectra taken with the 300 V and the 600 R grism, respectively (see Patat [2008]). Thus, we can also test our code in the optical regime and for low resolution. The resolution of the FORS spectra is about 500 and 1200, respectively, compared to values between 2000 and 5300 for the IR spectra. For each grism, the exposure dates and times of the target spectra were selected to differ from those of the fixed reference sky spectrum by the order of one hour and several years, respectively. The very long periods possible for the comprehensive FORS data set allow us to compare airglow spectra taken during phases of significantly different solar activity.

Since the task of the sky correction procedure is the subtraction of sky emission from an object spectrum showing a continuum and possible emission lines, a test that corrects one sky spectrum to fit another one is insufficient. Therefore, the sky spectra defined as science input were manipulated by adding an object spectrum (see Table 5). For this, best-fit spectral energy distributions (SEDs) of the nearby galaxies NGC 4594 and NGC 4625 obtained by means of the galaxy SED-fitting code CIGALE (see Noll et al. [2009]) were used. The spectra of the two NGC galaxies are very different. While NGC 4594 shows an early-type spectrum without significant emission lines, NGC 4625 is a late-type galaxy with strong emission lines. In order to move more lines and continuum features into a wavelength range where airglow is strong, the two galaxy SEDs were shifted to a redshift of $z = 0.5$. The flux of the object spectra was scaled arbitrarily. The SEDs were scaled such that they exhibit a similar strength as the airglow emission lines. Since the CIGALE model spectra were optimised to fit photometry (see Noll et al. [2009]), the resolution of the emission lines in the NGC 4625 spectrum is significantly lower than the resolution of our observed test sky spectra. In order to test the code for object emission lines having the same resolution as the sky lines (and to compensate for the lack of galaxy emission lines in the near-IR), we added 15 artificial lines of constant intensity to the NGC 4594 and NGC 4625 spectra. Lines were set at 0.5, 0.61, 0.71, 0.799553, 0.843248, 1.12, 1.153871, 1.19, 1.212263, 1.34, 1.50, 1.60, 1.670881, 1.700843, and 1.77 μm. Since the positions of 6 lines coincide with strong OH lines, the conservation of object line strength by the sky correction procedure can be investigated. The final object spectra were added to a representative subsample of the 11 target sky spectra defined as science input (see Table 4), which resulted in 2 × 5 different test set-ups with object spectrum (see Table 5).

For a better comparison of the results and to check the quality of the sky subtraction with standard parameters, we used identical input parameter files differing in the input and output file names and the selection of air or vacuum wavelengths only. The values of the fixed parameters can be found in the listing of the example parameter file shown in Section 4.1. The Tables 4 and 5 exhibit some results for each test set-up. First, the number of fit parameters is shown. The number of relevant A and B line group parameters (see Section 5.4) depends on the wavelength range covered by the spectra. Moreover, the rejection of unreliable lines can cause that line groups are not fittable and have to be scaled by mean factors (see Section 5.5). The number of coefficents of the Chebyshev polynomial for the wavelength grid correction (see Section 5.6) is variable, since an automatic search for the best degree is set by default (see Section 4.1). Then, the ranges of fitted line group flux correction factors are shown for the A and B groups. Note that the correction factors for lines groups of OH and O_2 can differ considerably. On the other hand, the range of scaling factors of groups of the same system (*e.g.* OH) can be significantly less spread than implied by the interval given in the table. As indicator for the quality of the sky correction procedure, Table 4 shows the weighted RMS derived from the difference between best-fit reference sky and input science line peak flux (no continuum) relative to the mean line peak flux in the science

	SKYCORR sky correction:	Doc:	VLT–MAN–ESO–19550–5896
ESO	User documentation and evaluation	Issue:	Issue 4.4
		Date:	Date 2014–04–01
		Page:	58 of 70

spectrum. Values in the order of a few per cent can be considered as good. Moreover, the mean ratio $\langle\frac{\Delta f_{\text{peak}}}{f_{\text{peak}}}\rangle$ of sky correction residual and line flux for a σ-clippped selection of fitted line peaks in the science spectrum is exhibited. This second quality measure can be compared to the relative RMS values. If it is distinctly lower, the RMS appears to be dominated by a few very strong residuals, since $\langle\frac{\Delta f_{\text{peak}}}{f_{\text{peak}}}\rangle$ is relatively insensitive to residuals that are much stronger than the average. For a visual inspection of the fit quality Figures 18 to 27 show several representative comparisons between best-fit sky and input science spectra. Finally, the results tables present the execution times of the sky line fit and the entire code for each set-up. For comparing the execution times, it should be noted that the X-Shooter spectra used have 16766 pixels, which is about an order of magnitude higher than the 2048, 1741, 1921, and 2041 pixels of the FORS, SINFONI *J*-band, SINFONI *H*-band, and SINFONI *K*-band spectra, respectively. Moreover, a degree of the optimal Chebyshev polynomial above the minimum degree of 3 of the iterative polynomial searching algorithm is related to a relatively long execution time, since for each additional degree the line fitting procedure has to be repeated (see Section 5.6).

6.2   Results

In general, the results of the sky correction procedure are satisfying. If only the results for sky spectra (without science object) as shown in Table 4 and Figures 18 to 23 are compared, the best fits are obtained for the first and third FORS set-up for which the tabulated RMS is below 1%. For these set-ups the time difference between both exposures is very short, *i.e.* in the order of one hour (see Table 3). However, even for combinations of spectra taken with several years in between the fits are good. The relatively low S/N of the X-Shooter spectra prevent better RMS values than those given in the table. Significant systematic residuals are rare. An example are the insufficently corrected O I multiplets at 777 and 845 nm of the first FORS set-up (see Figure 18). Usually these ionospheric lines are weak and difficult to detect among the strong OH lines. However, in the case of the target sky spectrum, a strong amplification of these lines occurred, which was much stronger than for the other ionospheric lines that mainly determine the correction of the A 3 group (see Table 1). Consequently, there are certain situations which impede a good correction of atomic lines originating in the thermosphere. However, the potentially affected wavelength ranges are very narrow. Another wavelength range which is difficult to correct is at about $1.27\,\mu\text{m}$. Figure 20 indicates conspicuous residuals there. The reason is the presence of a strong O_2 band (see Figure 16) with many overlapping lines at the resolution of SINFONI in the *J*-band. Hence, the continuum determination and the line group flux correction is very difficult in this wavelength range. For the case of the SINFONI example the correction was particularly challenging, since the intensities of the O_2(a-X)(0-0) band in the two input spectra differ by an extreme factor of about 7 (see Table 4). In contrast, the O_2 band correction worked much better for the X-Shooter spectra. The example shown in Figure 23 only indicates minor residuals. Reasons for the improved results are probably the lower correction factors (< 4) and the higher resolution (see Table 3). Finally, Figure 22 exhibiting the results of the SINFONI *K*-band set-up shows relatively strong residuals beyond $2.3\,\mu\text{m}$. Sky lines in the remaining spectrum are corrected very well. The emission lines at long wavelengths (beyond $2.3\,\mu\text{m}$) cannot be corrected by our sky subtraction code, since these are caused by thermal emission in the lower atmosphere and not airglow emission in the upper atmosphere. Consequently, the code does not scale line fluxes in the thermal IR. Note that a high degree of the Chebyshev polynomial for the wavelength grid correction could be a problem in this regime because of the required strong extrapolation. The example in Figure 22 does not seem to be affected by this issue. However, it shows that the subtracion of the strong thermal continuum, which is mainly caused by the telescope main mirror and cannot be fitted, can be a problem if the mirror temperature changes between the science and sky exposures.

Adding an object to the input science frame –quite expectedly– usually causes a decrease in the fit quality

(see Table 5). Nevertheless, in general, the resulting sky-subtracted spectra are good. Examples are shown in Figures 24 to 27. Due to a strong and complex continuum, it can happen that the line group correction factors become less reliable if the continuum has to be interpolated over a relatively wide wavelength range. This appears to be the reason for the relatively poor correction of the OH(9-4) band in the object FORS spectra shown in Figure 24 and 25 and the O_2(a-X)(0-0) band in the object SINFONI J-band spectra (see Figure 26). The X-Shooter spectra complemented by an object spectrum are much better corrected in this wavelength regime as a comparison of Tables 5 and 4 implies. Here, the relatively high resolution has probably helped to better constrain the continuum. Figures 24 to 27 illustrate the efficiency of SKYCORR in conserving the flux of object emission lines. The relatively broad lines of the galaxy spectra and the 5 narrow artificial lines (with FWHM matching that of the spectral set-up) are well conserved. Even lines directly positioned on top of airglow lines are regained almost perfectly. A requirement for such a good fit is that the object lines are masked by the σ-clipping approach described in Section 5.5. At least for the tested spectra the algorithm works very well.

The repeated fitting of airglow lines for different degrees of the Chebyshev polynomial for the wavelength grid correction (see Section 5.6) imposes a penalty on the code execution times. Run times from 4 to 97 s are tabulated in Tables 4 and 5. Most of this time is consumed by the iterative line fitting procedure. The code can be accelerated considerably by setting the parameter CHEBY_MAX to -1 (see Section 4.1). In this case, no wavelength correction is performed. This may be an option for spectra with very good wavelength calibration. However, if the wavelengths grids of two spectra indicate significant deviations, it is much better to perform the default fitting procedure. This is demonstrated by Figure 28 which shows the results of the fourth FORS set-up (see Table 4) without any wavelength correction. Compared to Figure 19 which exhibits the sky-subtracted spectrum for the standard run, the residuals in Figure 28 are extremely strong. The spectrum fors_0114, which was taken about four and a half years before the reference spectrum fors_1154 does not appear to be well calibrated. For example, the central wavelength of the O I line at 557.7 nm differs by about half a pixel. In this case a good wavelength grid correction is mandatory. This result justifies the choice of CHEBY_MAX = 7 and CHEBY_MIN = 3 for the standard run, which aims at providing acceptable sky-corrected spectra for all kinds of input data.

6.3 Comparison to Davies' code

For a concluding evaluation of the performance of SKYCORR, it is required to compare the present results to those of Davies' code, which is part of the SINFONI data reduction pipeline (see Section 2.1).

6.3.1 Results for the test set-up

A slightly adapted version of Davies' code was run on our test data set described in Section 6.1. The FORS set-ups have not been tested, since Davies' code is not able to correct airglow lines at wavelengths below 1 μm. Consequently, the resulting test data set consists of 7 pure sky and 8 object + sky set-ups. The results of the runs of both codes are summarised in Table 6. The listing exhibits the relative RMS mean values and their scatter for the subsample of pure sky spectra, the subsample of object spectra, and the total sample of 15 set-ups. In contrast to Tables 4 and 5, the RMS was computed for all pixels of the spectrum. Moreover, the RMS calculation is related to the difference between the residual of the sky correction and the input object spectrum which is a zero line for pure sky spectra. The RMS values of both codes are provided relative to the mean line peak flux in the input science spectrum. In order to simplify the comparison of the results of both codes, the ratio of

	SKYCORR sky correction:	Doc:	VLT–MAN–ESO–19550–5896
ESO	User documentation and evaluation	Issue:	Issue 4.4
		Date:	Date 2014–04–01
		Page:	60 of 70

Table 6: Comparison of SKYCORR and Davies' code

Sample[a]	$\frac{RMS_{\text{SKYCORR}}}{\langle f_{\text{peak}}\rangle}$ [b] [%]	$\frac{RMS_{\text{Davies}}}{\langle f_{\text{peak}}\rangle}$ [b] [%]	$\frac{RMS_{\text{SKYCORR}}}{RMS_{\text{Davies}}}$ [%]	$\frac{\langle|\Delta|\rangle_{\text{SKYCORR}}}{\langle|\Delta|\rangle_{\text{Davies}}}$ [c] [%]
Pure sky	3.9 ± 2.9	9.7 ± 8.0	47.4 ± 21.0	41.0 ± 15.4
Object + sky	4.8 ± 5.3	7.6 ± 7.8	60.4 ± 9.0	46.1 ± 6.2
All	4.4 ± 4.2	8.6 ± 7.7	54.3 ± 16.6	43.7 ± 11.3

[a] FORS spectra are not considered, since Davies' code cannot handle wavelengths below $1\,\mu$m.

[b] RMS (and its scatter) from difference between residual flux of sky correction by SKYCORR or Davies' code and pure object spectrum (zero line for pure sky spectra) relative to mean flux of science spectrum line peaks (flag $\geq$ 2; see Section 5.1). For the RMS, all pixels are considered except for wavelengths beyond $2.3\,\mu$m, where emission from the lower atmosphere dominates the spectra.

[c] Ratio of results of SKYCORR and Davies' code for mean absolute difference between residual flux of sky correction and pure object spectrum. Only wavelengths up to $2.3\,\mu$m are considered.
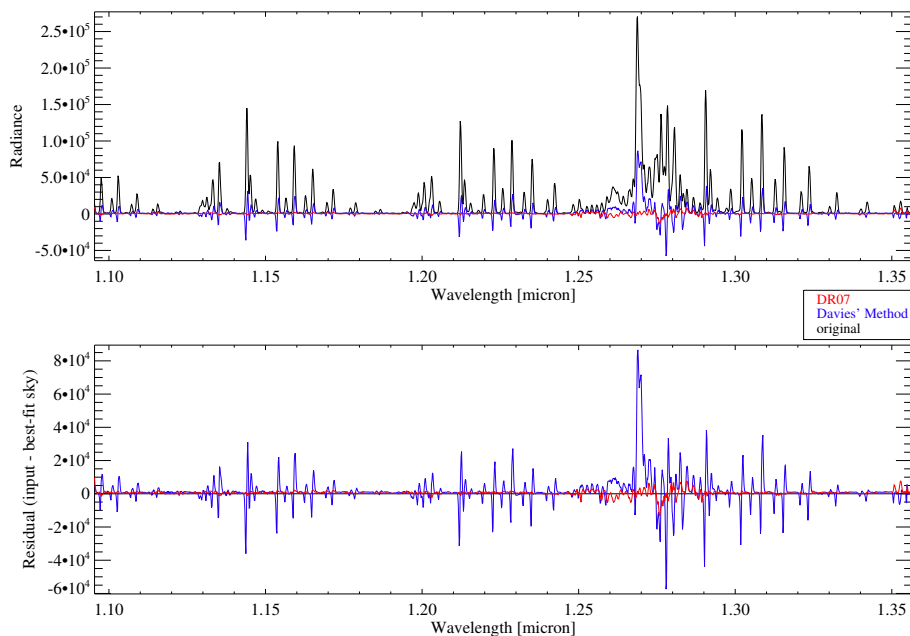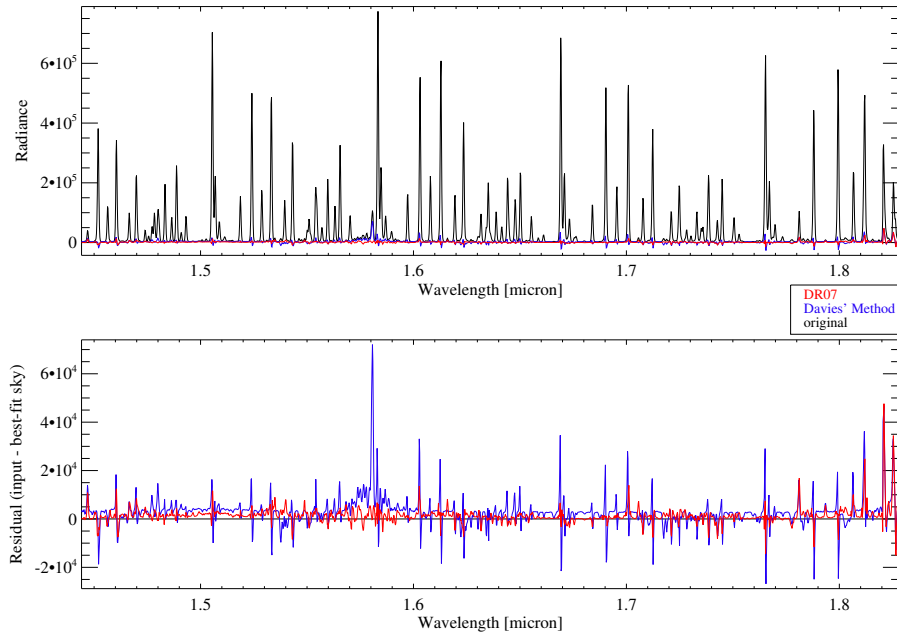

Figure 29: Comparison of SKYCORR (red) and Davies' code results (blue) for the SINFONI *J*-band set-up without object spectrum (cf. Figure 20). Apart from the residuals of the sky correction procedure the upper panel also shows the input science spectrum (black).
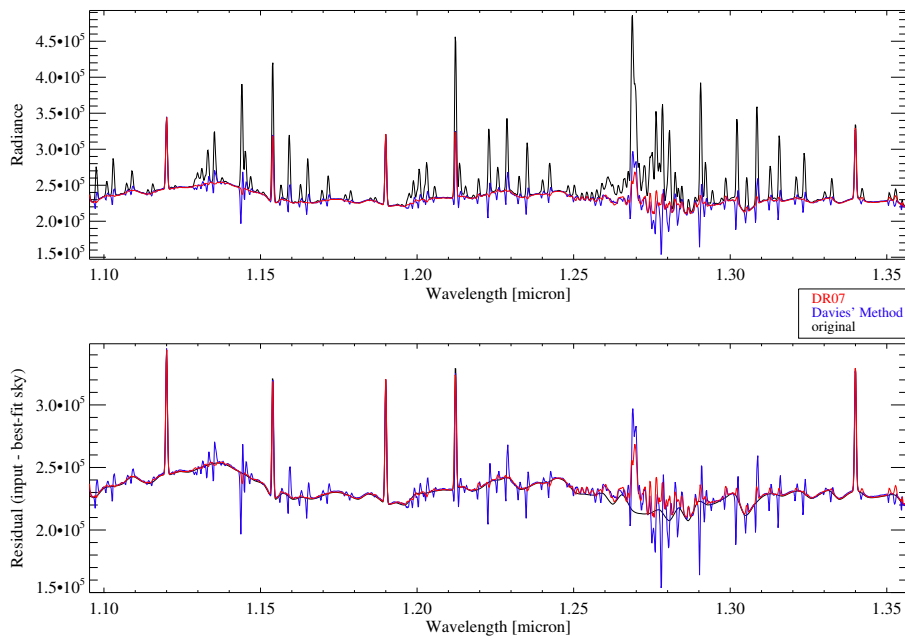
Figure 30: Comparison of SKYCORR (red) and Davies' code results (blue) for the SINFONI *H*-band set-up without object spectrum (cf. Figure 21). Apart from the residuals of the sky correction procedure the upper panel also shows the input science spectrum (black).

Figure 31: Comparison of SKYCORR (red) and Davies' code results (blue) for the SINFONI *J*-band set-up with object spectrum (cf. Figure 26). Apart from the residuals of the sky correction procedure the upper panel also shows the input science spectrum (black).

both RMS values is shown as well. Finally, a corresponding ratio for the mean absolute difference between sky correction residual and pure object spectrum is indicated. In comparison to the RMS ratio, the latter quantity is less sensitive to very strong residuals that affect a few pixels only. For this reason, a high RMS compared to the mean absolute difference suggests that strong residuals affect a relatively narrow range of the spectrum only. Examples for the differences in the results of both codes are presented in Figures 29 to 31.

Table 6 indicates that SKYCORR has an improved performance in comparison to Davies' code. In the tested set-ups, the RMS of SKYCORR is lower. On average the RMS ratio is about 54%. For pure sky spectra, the results tend to be better than for science spectra incorporating an object (47% versus 60%). This discrepancy is not observed for the mean absolute difference, where the results for the two subsamples differ from the mean of 44% only slightly. The differences in the results for both quantities can be explained –as already mentioned above– by the dominance of the contribution to the RMS by a few residual pixels. Such a situation is shown in Figure 31, which indicates relatively strong residuals for the O_2 band at 1.27 μm. Apart from the O_2 band, where both codes are comparable, the SKYCORR performance is superior (by a factor of 2 on average). However, this particular band cannot be corrected very well, since the density of strong lines is very high requiring interpolation of the continuum over a relatively wide wavelength range. As already discussed in context of Figure 20, the interpolation, the complex object continuum, and the extreme difference in the properties of the two sky spectra, prevent a good sky correction in this wavelength range.

6.3.2   Results for SINFONI pipeline data

For the code evaluation by means of sky model verification data and simulated object spectra (see Section 6.3.1), Davies' code was modified to handle data that was not processed with this routine before. In order to get a better idea how SKYCORR would perform if it was used in the SINFONI pipeline (Modigliani et al. [2007]) instead of the Davies method, one could also modify the SINFONI pipeline products to allow an application of SKYCORR. For this purpose, suitable object and reference sky 1D data derived from SINFONI data cubes for spectroscopic observations in different bands were provided by A. Modigliani from ESO.

In Figures 32 to 34, we illustrate the performance of SKYCORR for this realistic data set comprising observations in the *H*, *K*, and *HK*-band modes. The results are superb for *H* and *K* with relative residuals of about three orders of magnitude weaker than the original airglow lines. Moreover, the comparison to the Davies code indicates a significantly better sky subtraction by SKYCORR, which is in agreement with the results of Section 6.3.1. The results of the *HK* mode are worse for both codes with residuals up to several per cent. For the default parameter set-up, the quality of the SKYCORR sky-subtracted spectrum is relatively similar to the one produced by Davies' code. However, the wavelength position and shape of the residuals are very different. As demonstrated by Figure 34, an optimisation of the SKYCORR input parameter set can distinctly improve the results. To achieve the convincing sky subtraction, only the MIN_LINE_DIST parameter (see Section 4.2) was set from 2.5 to 12.5. Likewise, another good result was obtained by changing FLUXLIM from -1 to 0.08. These changes affect the line finder (Section 5.1) and the separation of lines and continuum (Section 5.3). This makes sense, since the resolution of the SINFONI *HK*-band mode is relatively low (about 1500; cf. Table 3), which causes enhanced line blending. Hence, the line detection and continuum separation becomes difficult if pseudo continua consisting of line blends cover large parts of the investigated spectrum. In particular, the *H* band around the O_2 band at 1.58 μm characterised by a high line density (see Figure 17) appears to be affected by this issue.

Summarising the evaluation section, we can conclude that the SKYCORR sky correction code produces con-
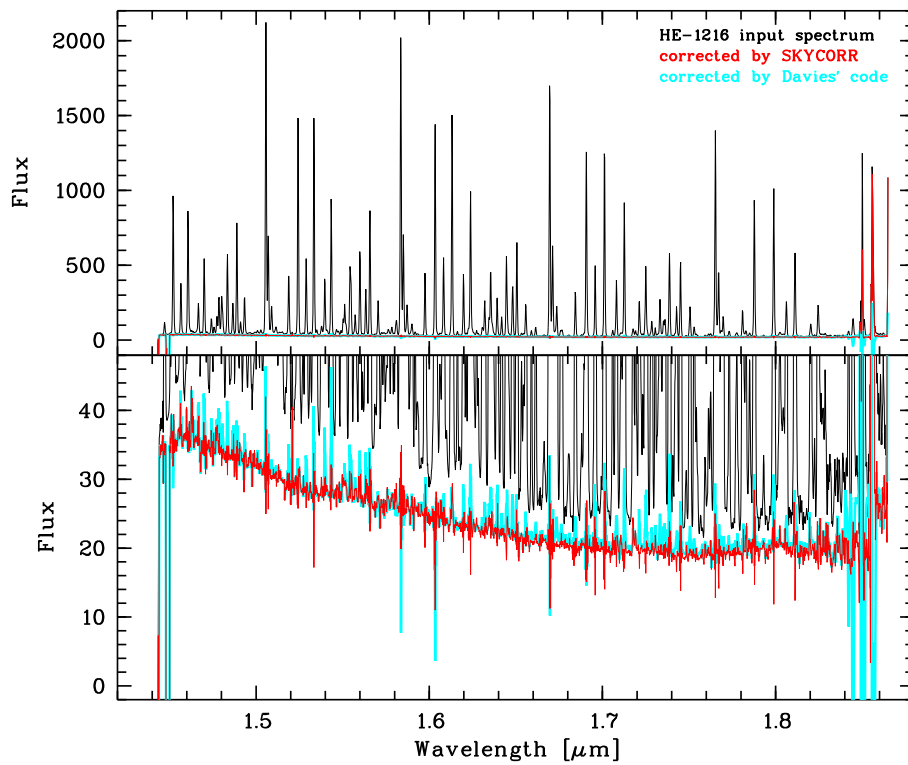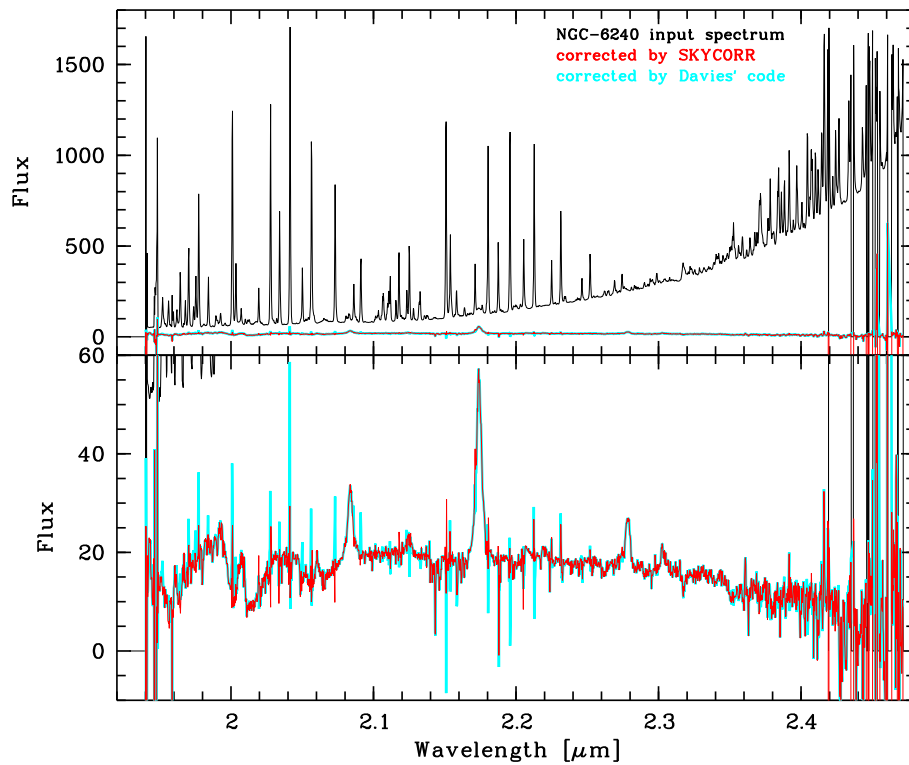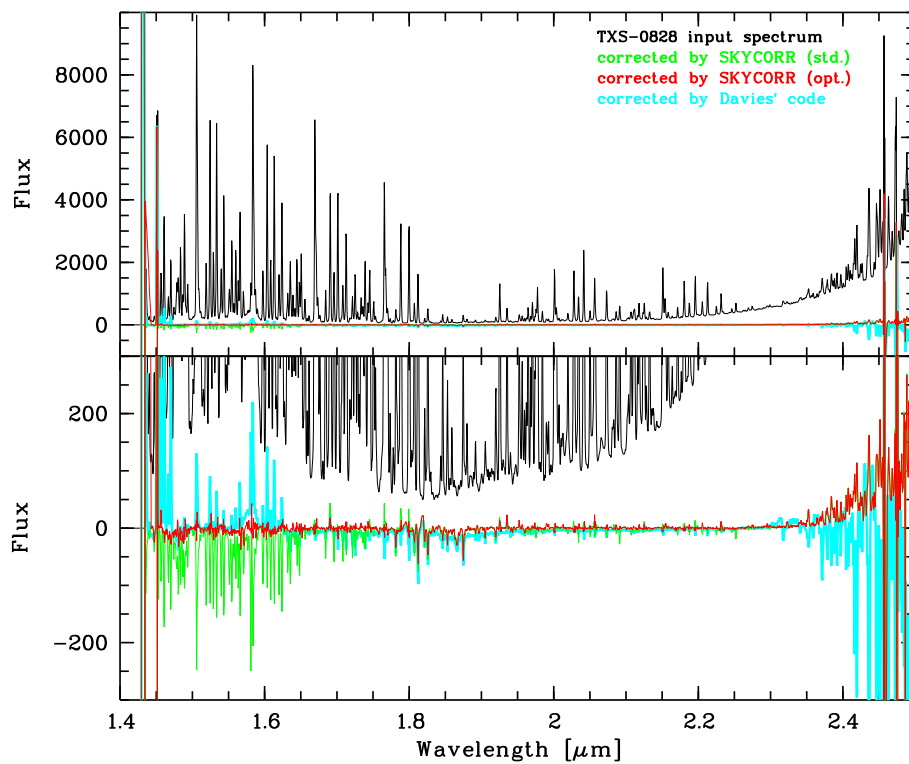
Figure 32: Comparison of SKYCORR (red) and Davies' code results (cyan) for a SINFONI *H*-band pipeline product. While the upper panel shows the full input spectrum of HE 1216, the lower panel focuses on the sky subtraction results.

Figure 33: Comparison of SKYCORR (red) and Davies' code results (cyan) for a SINFONI *K*-band pipeline product. While the upper panel shows the full input spectrum of NGC 6240, the lower panel focuses on the sky subtraction results.

Figure 34: Comparison of SKYCORR (green/red) and Davies' code results (cyan) for a SINFONI *HK*-band pipeline product. SKYCORR was run for the default parameter set (green; see Section 4.1) and an optimised set-up (red), which only differs from the standard by MIN_LINE_DIST = 12.5. While the upper panel shows the full input spectrum of TXS 0828, the lower panel focuses on the sky subtraction results.

vincing results for various kinds of data even if the time period between the object and reference sky exposures is very long. In general, the results are better than those produced by Davies' code. In most cases, good sky subtraction can be achieved with a minimum of interaction. If this is not sufficient, the user can try to fine-tune the sky subtraction by varying the procedure's input parameters (see Section 4.2). Also, this will influence the code run time.

Acronyms

ASCII American Standard Code for Information Interchange

CPL Common Pipeline Library

ESO European Southern Observatory

FITS Flexible Image Transport System

FORS FOcal Reducer and low dispersion Spectrograph

FWHM full width at half maximum

GUI Graphical User Interface

HITRAN High-resolution transmission molecular absorption database

IDL Interactive Data Language

IR infrared

ISAAC Infrared Spectrometer and Array Camera

LBLRTM Line-by-line Radiative Transfer Model

RMS root mean square

SED spectral energy distribution

sfu solar flux units

SINFONI Spectrograph for INtegral Field Observations in the Near Infrared

S/N signal-to-noise ratio

UVES Ultraviolet and Visual Echelle Spectrograph

VIMOS Visible Multi-Object Spectrograph

VLT Very Large Telescope

References

[2005] Clough, S.A, Shephard, M.W., Mlawer. E.J., et al. 2005, J. Quant. Spectrosc. Radiat. Transfer, 91, 233

[2006] Cosby, P.C., Sharpee, B.D., Slanger, T.G., Huestis, D.L., & Hanuschik, R.W. 2006, J. Geophys. Res., 111, A12307

[2007] Davies, R.I. 2007, MNRAS, 375, 1099

[1998] Goldman, A., Schoenfeld, W.G., Goorvitch, D., et al. 1998, J. Quant. Spectrosc. Radiat. Transfer, 59, 453

[2003] Hanuschik, R.W. 2003, A&A, 407, 1157

[2008] Khomich, V.Y, Semenov, A.I., & Shefov, N.N. 2008, Airglow as an Indicator of Upper Atmospheric Structure and Dynamics, Springer, Berlin

[1974] Mies, F.H. 1974, J. Molec. Spectrosc., 53, 150

[2007] Modigliani, A., Hummel, W., Abuter, R., et al. 2007, The SINFONI pipeline, arXiv:astro-ph/0701297

[2010] Modigliani. A., Goldoni, P., Royer, F., et al. 2010, Proc. SPIE, 7737, 773728

[1980] Moré, J.J., Garbow, B.S., & Hillstrom, K.E. 1980, User Guide for MINPACK-1, Argonne National Laboratory Report ANL-80-74, Argonne, Ill.

[2009] Noll, S., Burgarella, D., Giovannoli, E., et al. 2009, A&A, 507, 1793

[2012] Noll, S., Kausch, W., Barden, M., et al. 2012, A&A, 543, A92

[2008] Patat, F. 2008, A&A, 481, 575

[2009] Rothman, L.S., Gordon, I.E., Barbe, A., et al. 2009, J. Quant. Spectrosc. Radiat. Transfer, 110, 533

[2000] Rousselot, P., Lidman, C., Cuby, J.-G., Moreels, G., & Monnet, G. 2000, A&A, 354, 1134

[SM-01] SM-01 User Manual, VLT-MAN-ESO-19550-5770

[MOLECFIT] MOLECFIT User Manual, VLT-MAN-ESO-19550-5772

[SM-SoW] Statement of Work for SM projects, VLT-SOW-ESO-19550-5223

[SM-03-SR] SM-03 Science Report, VLT-TRE-ESO-19550-5775

[Reflex-UM] Reflex User Manual, VLT-MAN-ESO-19000-5037

Links

[1] `http://www.physics.wisc.edu/ craigm/idl/cmpfit.html`

[2] `http://www.aer.com/`

[3] `http://www.cfa.harvard.edu/HITRAN/`

[4] `http://www.astro.washington.edu/docs/idl/htmlhelp/slibrary30.html`

[5] AMC Technical Briefs - ISSN 1757-5958, No.6, Royal Society of Chemistry, 2001, `http://www.rsc.org/images/brief6_tcm18-25948.pdf`

[6] `http://rtweb.aer.com/lblrtm_frame.html`

[7] `http://www.eso.org/sci/software/cpl`

— End of document —